

# Novel vascular disrupting agents with a cyclohexanedione scaffold identified through a ligand-based virtual screening approach

*María-Dolores Canela,<sup>#</sup> María-Jesús Pérez-Pérez<sup>#</sup>, Sam Noppen,<sup>†</sup> Gonzalo Sáez-Calvo,<sup>◇</sup> J.  
Fernando Díaz,<sup>◇</sup> María-José Camarasa,<sup>#</sup> Sandra Liekens<sup>†\*</sup> and Eva-María Priego<sup>#\*</sup>*

<sup>#</sup> Instituto de Química Médica (IQM-CSIC), Juan de la Cierva 3, E-28006 Madrid, Spain

<sup>†</sup> Rega Institute for Medical Research, KU Leuven, B-3000 Leuven, Belgium.

<sup>◇</sup> Centro de Investigaciones Biológicas (CIB-CSIC), Ramiro de Maeztu 9, E-28040 Madrid, Spain

TITLE RUNNING HEAD: Vascular disrupting agents based on cyclohexanediones

CORRESPONDING AUTHOR FOOTNOTE

Eva-María Priego

Instituto de Química Médica (CSIC)

Juan de la Cierva 3, 28006 Madrid (Spain)

Phone: +34 91 5680040

Fax: 34 91 5644853

e-mail: [empriego@iqm.csic.es](mailto:empriego@iqm.csic.es)

Sandra Liekens

Rega Institute for Medical Research, KU Leuven

Minderbroedersstraat 10, blok x – bus 1030, B-3000 Leuven, Belgium

Phone: +32 (0) 16337355

Fax: +32 (0) 16337340

e-mail: [sandra.lieken@rega.kuleuven.be](mailto:sandra.lieken@rega.kuleuven.be)

Abbreviations: VDA: vascular-disrupting agent; VS: virtual screening; ROCS: rapid overlay of chemical structures; MTC: 2-methoxy-5-(2,3,4-trimethoxyphenyl)-2,4,6-cycloheptatrien-1-one; R-PT: (R)-(+)-ethyl 5-amino 2-methyl-1,2-dihydro-3-phenylpyrido[3,4-*b*]pyrazin-7-yl carbamate.

## ABSTRACT.

Vascular Disrupting Agents (VDAs) constitute an innovative anticancer therapy that targets the tumor endothelium, inducing crucial morphological and functional changes that trigger a rapid and dramatic decrease in blood flow leading to tumor necrosis. Our approach for the identification of new VDAs has relied on a ligand 3-D shape similarity virtual screening (VS) approach using as query agents that bind the  $\alpha,\beta$ -tubulin dimer at the colchicine-binding site. The VS campaign, followed by biological testing, afforded an interesting hit with a cyclohexane-1,3-dione structure. This was followed by a synthetic programme of structural analogues. Interestingly, several of these new analogues showed anti-proliferative activity in the sub- $\mu$ M range, being 100-fold more potent than the initial hit. Additional biological assays showed that they arrest the cell cycle at the G2/M phase and bind at the colchicine-binding site in tubulin with binding affinities in the low- $\mu$ M range. Moreover, these compounds cause vascular disruption as shown by their ability to destroy an established endothelial tubular network. In conclusion, our approach has led to a new family of promising anti-proliferative compounds with antimitotic and VDA properties.

**KEYWORDS:** virtual screening; vascular-disrupting agents; colchicine; cyclohexanediones

## Introduction

The growth of solid tumors and development of metastasis are highly dependent on the existence of a vascular network that provides oxygen and nutrients.<sup>1</sup> Therefore anti-vascular strategies are increasingly gaining importance among anti-neoplastic therapies and represent a new frontier in the treatment of cancer.<sup>2</sup> Basically, there are two major approaches in anti-vascular therapies: anti-angiogenic drugs, which inhibit new blood vessel formation,<sup>3</sup> and vascular-disrupting agents or VDAs, which affect the existing vasculature.<sup>4,5</sup> While anti-angiogenic drugs are mostly cytostatic to the endothelial cells and need to be chronically administered, VDAs are typically cytotoxic and cause a quick and dramatic collapse in the blood flow that leads to ischemia and necrosis just 24 h after administration. Thus, they are particularly effective in advanced stages when large tumors are formed. Importantly, one of the main advantages of such anti-vascular approaches is that they target endothelial cells, a cell population less prone to mutations than tumor cells.<sup>6</sup>

The selectivity of VDAs for tumor endothelium versus physiological vessels lies in the crucial differences between them.<sup>7</sup> In fact, tumor vessels are characterized by a higher proliferation rate, absence of pericytes, basal membrane deficiencies and increased vascular permeability. Moreover, tumor vessels are more fragile and tortuous which results in a higher resistance to blood flow. This makes them more sensitive to any decrease in perfusion pressure.<sup>8</sup>

Besides biotechnological approaches, involving immunotoxins and targeted antibodies, there is an increasing interest in low-molecular-weight molecules that behave as VDAs, and some of them are in clinical trials for a variety of solid tumors.<sup>9</sup> The best studied VDAs are microtubule-destabilizing agents that bind the  $\alpha,\beta$ -tubulin dimer at the colchicine-binding site.<sup>10</sup> The most representative compounds include colchicine (**1**), ZD6126 (**2**), ABT-751 (**3**), combrestatins and their prodrugs, CA1P (**4**), CA4P (**5**) and AVE-8062 (**6**), as shown in Figure 1. These compounds inhibit tubulin polymerization in endothelial cells affecting the cellular cytoskeleton and therefore induce changes not only in the shape of endothelial cells but also in their motility, invasion, attachment and proliferation.<sup>11,12</sup> As a result of a large cascade of events, such as actin stress fiber contraction and the subsequent activation of Rho kinases, VDAs lead to vascular collapse, tumor hypoxia and hemorrhagic necrosis.<sup>13</sup>

It is interesting to mention that colchicine-like VDAs are able to behave as anti-mitotic agents at concentrations slightly higher than those at which the anti-vascular effects are observed. This anti-mitotic effect, closely related to the importance of the cytoskeleton of  $\alpha,\beta$ -tubulin in mitotic spindle formation, when

affecting tumor cells, may induce apoptosis. Therefore, this dual mechanism of action affecting endothelial and tumor cells makes these drugs very promising for anti-cancer therapy.<sup>14</sup>

Despite the great potential of these drugs, they suffer some drawbacks. In particular, colchicine is too toxic to be considered a suitable anti-cancer drug<sup>15</sup> and CA-4P presents chemical instability leading to the inactive trans-isomer and shows a short biological half-life.<sup>16</sup>

Therefore our objective has been to identify new chemical entities able to bind at the colchicine-binding site in  $\alpha,\beta$ -tubulin that may lead to a novel type of compounds with anti-proliferative and anti-vascular properties. To address this aim, we relied on a ligand-based virtual screening (VS) approach.<sup>17</sup> Such approach represents a quick, efficient and well-documented strategy to access novel active molecules for a particular target. Among the computational methods available for this strategy, we have focused on 3-D shape similarity, a strategy successfully applied on recently reported examples.<sup>18</sup> A significant advantage of this approach is that no specification of the chemical structure (i.e. types of atoms and/or their bond arrangements) is required, thus chemical scaffolds significantly different from the template can be identified.

Here we report the results obtained after conducting a ligand-based VS campaign using two different queries, identification of the hits and further exploration in terms of improvement of their anti-proliferative properties and determination of the mechanism of action.

## **Results and Discussion**

### **Virtual screening**

The Virtual Screening protocol employed is summarized in Figure 2 and all details are described in the Experimental Section.

The compounds for the virtual screening were obtained from the freely available ZINC database,<sup>19</sup> (version 8, which comprises about 8.5 million molecules) in SMILES format.<sup>20</sup> Prior to VS, the database was filtrated on the basis of a customized “drug-like filter” using the software FILTER,<sup>21</sup> to remove, among others, compounds with reactive functional groups. The filtered database was subjected to OMEGA<sup>22</sup> to generate the 3D atomic coordinates and conformational ensembles of all the compounds. As tool for the VS, we have used ROCS,<sup>23</sup> a shape comparison program based on the concept that molecules have a similar shape if their volumes, represented by a Gaussian function, overlay well.<sup>24,25</sup> Besides shape comparison, an electrostatic complementary term called “color”, which represents chemical similarity, was also applied.

As query against which the comparison was performed, the 3-D structure of two well-known tubulin binders at the colchicine site was used: a colchicine derivative (DAMA-colchicine, **7**)<sup>26</sup> and TN-16 (**8**)<sup>27</sup> (Figure 3A). A superposition of their experimental cocrystal structures with  $\alpha,\beta$ -tubulin is shown in Figure 3B. The X-Ray of the complex tubulin-TN-16, reported in 2009, clearly shows that this compound is more deeply buried in the  $\beta$ -monomer than DAMA-colchicine, so that it explores a pocket partially different to that of colchicine.<sup>27</sup>

The VS protocol included shape comparison and scoring, “color” comparison and scoring (shape plus color) and finally visual inspection. Based on previously reported examples,<sup>25</sup> we established a Tanimoto score of 0.75 for the shape comparison, and a “Combo-score” of 1.4 for the sum of shape and color comparison.

When using DAMA-colchicine as query, the highest hits in the scoring list showed structures that closely resembled colchicine or other described tubulin inhibitors, thus no novel scaffolds were identified. Alternatively, when TN-16 was used as template, the scoring list revealed nine clusters of compounds that had not been previously described in the literature as tubulin binders. Based on compound availability, a total of six representative examples of these clusters (see Table S1 in the Supporting Information) were purchased and evaluated for their anti-proliferative activity against one endothelial cell line (, MBEC) and one tumor cell line (L1210). From the compounds tested, only the cyclohexanedione **9** (Figure 4) showed significant inhibition of cell proliferation in both cell lines with  $IC_{50}$  values of  $13 \pm 5 \mu M$  (Table S2 in the Supporting Information). Evaluation of **9** against other four cell lines indicated similar  $IC_{50}$  values. In addition binding of the hit compound **9** to tubulin at the colchicine-site was confirmed by the displacement of 2-methoxy-5-(2,3,4-trimethoxyphenyl)-2,4,6-cycloheptatrien-1-one (MTC, a reversible colchicine-binding site ligand) as determined by fluorescence spectroscopy (see Figure S1 in the Supporting Information). Moreover, and from a chemical point of view, compound **9** was considered a suitable hit based on its low molecular weight (335), and synthetic accessibility as described in the next section. Therefore a synthetic-driven medicinal chemistry program was set up to evaluate structural analogues of **9**.

## Chemistry

Since the hit compound **9** had been acquired from a commercial source, the first task was to devise a synthetic strategy that could allow the exploration of the different fragments of the molecule (Figure 4), in

particular the aromatic rings **A** and **D**, and the alkyl chain **C**, while keeping the cyclohexanedione **B** as a common structural motif. This strategy consisted in the reaction of the 5-substituted cyclohexane-1,3-diones (representing fragments **A** and **B**) with acyl chlorides to obtain the *C*-acyl derivatives followed by Schiff base formation with anilines (fragment **D**). Since fragment **D** was the last structural element incorporated in this synthetic strategy, the first series of modifications were performed on this fragment.

Thus, reaction of the commercially available 5-phenylcyclohexane-1,3-dione (**10**) with propionyl chloride in dichloromethane in the presence of DMAP and DIPEA at 70 °C (Scheme 1) as described for similar analogues<sup>28</sup> afforded the *O*-acyl derivative **11** in 64% yield, but not the *C*-acyl derivative **12** as expected. Interestingly, similar *O*-acyl derivatives have been transformed into the corresponding *C*-isomers by reaction with K<sub>2</sub>CO<sub>3</sub> in acetonitrile in the presence of 1,2,4-triazole, by varying the temperature between -10 and 100 °C, or by phase-transfer catalysis.<sup>29</sup> When compound **11** was treated with K<sub>2</sub>CO<sub>3</sub> in acetonitrile in the presence of 1,2,4-triazole at 30 °C, only 30% of the *C*-analogue **12** was obtained after 48 h of reaction. However, with this information, we assayed new reaction conditions meant to perform these two steps in a “one-pot” procedure, and making use of microwave-assisted irradiation to reduce the reaction times. Thus, reaction of **10** with propionyl chloride in CH<sub>3</sub>CN under microwave conditions in the presence of K<sub>2</sub>CO<sub>3</sub>, 1,2,4-triazole and Bu<sub>4</sub>NBr as a phase transfer catalyst at 70 °C afforded the corresponding *C*-propionyl derivative **12** in 51% yield. It should be mentioned that the combination of phase transfer catalysis and microwave irradiation afforded the desired *C*-acyl derivative in just a couple of hours, and to the best of our knowledge, this methodology has never been applied to this type of reaction.

Then reaction of **12** with anilines carrying OH or OMe groups in toluene at 150 °C for 2 h under microwave radiation in the presence of 4Å molecular sieves yielded compounds **14a-j**. The structures of **14a-j** were determined by <sup>1</sup>H NMR, <sup>13</sup>C NMR, HMBC and HSQC correlation experiments. It should be emphasized that, in the <sup>1</sup>H NMR spectra, a broad singlet appeared around 15 ppm corresponding to the NH group. This chemical shift suggested the participation of the NH in a potential hydrogen bond with one of the carbonyl groups of the 1,3-cyclohexanedione. To further explore this issue, the <sup>1</sup>H NMR spectra of compound **14c** was recorded in DMSO-*d*<sub>6</sub> and CDCl<sub>3</sub>, and in both cases the NH signal remained almost unaffected (δ 14.7 ppm). Additionally, a ten-fold dilution of the sample with DMSO-*d*<sub>6</sub> did not affect the chemical shift of this signal, strongly suggesting the existence of an intramolecular hydrogen bond.

When tested for anti-proliferative activity (see Table 1, Biological Evaluation section), compounds **14c** and **14j** afforded 2- to 30-fold lower IC<sub>50</sub> values than the initial hit **9**. Therefore, we decided to explore the length of the alkyl chain in fragment **C** while keeping an OMe or Me in *ortho* at the **D** aromatic ring (Scheme 2). Thus, reaction of the cyclohexanedione **10** with butyryl or acetyl chloride in the presence of K<sub>2</sub>CO<sub>3</sub>, 1,2,4-triazole, Bu<sub>4</sub>NBr in acetonitrile under microwave conditions afforded the *C*-acyl derivatives **15a** and **15b**, respectively. Further reaction of these acyl derivatives with *o*-toluidine or *o*-anisidine in toluene afforded compounds **16a-d** in excellent yields.

As will be later discussed (Biological Evaluation section), those compounds with a methyl at fragment **C** afforded the best inhibitory values. With this information, and keeping a methyl as side chain in **C**, a wider battery of anilines was introduced at fragment **D** with at least one substituent at position 2 of the aromatic ring. Therefore, as shown in Scheme 3, reaction of 2-acetyl-5-phenylcyclohexane-1,3-dione (**15b**) with commercially available 2-chloro (**17a**), 2-fluoro (**17b**), 2-trifluoromethyl (**17c**), 2,3-difluoro (**17d**), 2,6-difluoro (**17e**), 2,5-dimethoxy (**17f**) and 2,6-dimethoxy (**17g**) anilines afforded compounds **18a-g**.

The next series of modifications affected fragment **A** by replacing the phenyl ring by other groups, in particular, a cyclohexyl, a benzyl or a *gem*-dimethyl (Scheme 4). The cyclohexane-1,3-diones with a cyclohexyl or a benzyl at position 5 (**21a** and **21b**) were synthesized through the  $\alpha,\beta$ -unsaturated ketone precursors (**20a** and **20b**) that were obtained following two different approaches. The synthesis of **20a** was undertaken by condensation between cyclohexane carbaldehyde (**19a**) and acetone under basic conditions,<sup>30</sup> while the benzyl derivative **20b** was obtained by a Wittig reaction of phenylacetaldehyde (**19b**) with 1-(triphenylphosphoranylidene)-2-propenone in chloroform following described procedures.<sup>31</sup> Then **20a** and **20b** were allowed to react with diethylmalonate in the presence of sodium ethoxide in ethanol at 60 °C<sup>30</sup> to afford the cyclohexane-1,3-diones **21a** and **21b**, respectively. *C*-acylation of **21a** and **21b** with acetyl chloride, as described in previous examples, and further reaction with *o*-anisidine afforded **23a** and **23b** in excellent yields. Similarly, reaction of the commercially available *gem*-dimethyl derivative **22c** with *o*-anisidine in toluene at reflux afforded **23c**. It should be mentioned that these compounds were poorly active, pointing to the importance of the aromatic ring directly attached to the cyclohexanedione for the anti-proliferative activity.

Thus, keeping a phenyl group at **A**, a variety of substituents were introduced at this ring. The 5-phenylcyclohexane-1,3-diones **24a-h** (Scheme 5) were synthesized from the corresponding substituted benzaldehydes following described procedures,<sup>32,33</sup> in a similar way to that described in Scheme 4. *C*-



acylation of **24a-h** with acetyl chloride and further reaction with *o*-anisidine or *o*-toluidine provided compounds **26a-k**. Finally, demethoxylation of **26k** with BBr<sub>3</sub> in CH<sub>2</sub>Cl<sub>2</sub> at room temperature afforded the corresponding hydroxyl derivative **26l**.

## Biological Evaluation

### Anti-proliferative activity

The synthesized compounds were evaluated for their anti-proliferative activity in six different cell lines: three endothelial cell lines [human microvascular endothelial cells (HMEC-1), mouse brain endothelial cells (MBEC) and bovine aortic endothelial cells (BAEC)] and three cancer cell lines [mouse lymphocytic leukemia (L1210), human lymphoblastic leukemia (CEM) and human cervical carcinoma (HeLa) cells].<sup>34</sup> Data are expressed as IC<sub>50</sub> (50% inhibitory concentration) defined as the concentration at which the compounds reduce cell proliferation by 50% and are shown in Table 1. As reference compound we included colchicine (**1**), which inhibited proliferation of the different cell lines with IC<sub>50</sub> values ranging from 0.0038 to 0.031 μM.

Those compounds with an OH at position *orto*, *meta* or *para* in fragment **D** (**9**, **14a** or **14b**) were moderately active in the different cell lines with IC<sub>50</sub> values ranging from 8 to 36 μM in endothelial cells, and from 11 to 79 μM in the tumor cell lines. However, compounds with an OMe at these positions showed a more diverse behavior in terms of anti-proliferative activity. Thus, the *p*-OMe compound (**14e**) was marginally active in some cell lines (IC<sub>50</sub> ≥ 57 μM), the *m*-OMe derivative (**14d**) showed moderate activity (IC<sub>50</sub> of 16-66 μM) while the *o*-OMe isomer (**14c**) afforded IC<sub>50</sub> values of 1.2-4.3 μM, that is, 10- to 30-fold better than the hit compound **9** in endothelial cells. The double or triple substituted compounds (**14f**, **14g** or **14h**) were inactive or poorly active. The unsubstituted compound (**14i**) showed moderate anti-proliferative activity while the *o*-CH<sub>3</sub> derivative (**14j**) was as active as the corresponding *o*-OMe compound **14c**.

The length of the alkyl chain in fragment **C** was varied while keeping an OMe or Me in *orto* at the **D** aromatic ring. The resulting propyl derivatives **16a** and **16b** showed moderate anti-proliferative activity with IC<sub>50</sub> values at least 13-fold higher than those of the corresponding ethyl derivatives **14c** and **14j**. Interestingly, the methyl derivatives **16c** and **16d** were significantly more active than the corresponding ethyl derivatives, with IC<sub>50</sub> values as low as 0.09 μM and 0.18 μM for compound **16c** in endothelial and tumor cells, respectively. Depending on the cell line, this represents a 60- (Hela cells) to 400-fold (BAEC) increase in the

anti-proliferative effect compared with the initial hit. Thus a methyl was selected as the substituent of choice in fragment **C**.

Keeping a methyl group as the alkyl chain at fragment **C**, we further explored the *orto* position in fragment **D** incorporating different electron withdrawing groups. Thus, introduction of a chlorine (**18a**) afforded IC<sub>50</sub> values in the sub- $\mu$ M range (0.3-0.7  $\mu$ M), whereas a fluorine (**18b**) resulted in slightly increased IC<sub>50</sub> values (0.5-3.4  $\mu$ M) and the *o*-trifluoromethyl derivative **18c** lost 10-fold activity (IC<sub>50</sub> of 8-32  $\mu$ M). Interestingly, the disubstituted derivatives (2,3-difluor (**18d**), 2,6-difluor (**18e**) and 2,5-dimethoxy (**18f**)) were all moderate inhibitors of cell growth, being less potent than the related *orto*-monosubstituted compounds (i.e **18b** and **16c**, respectively) whereas the 2,6-dimethoxy derivative (**18g**) showed comparable activity as **18b**.

Concerning fragment **A**, substitution of the phenyl ring by a cyclohexyl (compare **16c** and **23a**) resulted in at least 10-fold higher IC<sub>50</sub> values. Replacement by a benzyl or a gem-dimethyl (compounds **23b** and **23c**) was even more detrimental for activity, suggesting the importance of an aromatic ring directly attached to the cyclohexane-1,3-dione. Finally, we introduced a variety of substituents at this phenyl ring (compounds **26a-l**, Table 1). Compounds substituted with Me or F at *orto* in fragment **A** (**26a** and **26b**) showed some anti-proliferative activity against the different cell lines, but at IC<sub>50</sub> values 50-fold higher than the unsubstituted phenyl derivative **16c**. Introduction of a double substitution at 2 and 6 either with methyl or fluorine (**26c** and **26d**, respectively) reduced the anti-proliferative effect even more. On the other hand, the *meta*-substituted compounds **26e**, **26f** and **26k** were nicely active in all cell lines with IC<sub>50</sub> values around 0.17-0.79  $\mu$ M. Only compound **26l**, with an OH at *meta*, was less active with an IC<sub>50</sub> value in the low- $\mu$ M range. Finally, the *para*-substituted compounds showed only very moderate anti-proliferative activity, the only exception being **26j**, containing a fluorine, that was still 20-fold less active than the unsubstituted compound **16c**.

From this evaluation some structural requirements for anti-proliferative activity among this family of compounds can be extracted: (i) the aromatic ring **D** needs to be substituted at the *orto* position with either a methoxy, a methyl, a Cl or to a lesser extend a F; (ii) the optimal alkyl chain at fragment **C** seems to be one carbon atom; (iii) fragment **A** must be a phenyl, preferentially unsubstituted or with a methyl or methoxy at *meta*.

A number of *in vitro* experiments were then carried out to elucidate the mechanism of action of these new anti-proliferative compounds. Colchicine was included as positive control.

### **Inhibition of Cell Cycle Progression.**

To investigate at which phase of the cell cycle the compounds exert their anti-mitotic effect, we performed cell cycle analysis on HMEC-1 treated with 6 of the most potent compounds (**16c**, **16d**, **18a**, **18b**, **26e** and **26f**).<sup>35</sup> Thus, HMEC-1 were incubated in the presence of different concentrations of colchicine or tested compound for 24 hours, after which cell cycle distribution was measured by flow cytometry. The results obtained for compounds **16c**, **16d** and colchicine (**1**) are shown in Fig 5. Untreated cells showed a classical pattern of proliferating cells distributed in the G1, S and G2/M phase. When these cells were treated with 0.03  $\mu$ M colchicine, an accumulation in G2/M phase and an increase in subG1 cells undergoing apoptosis, was observed. The same effect was noted in the presence of the tested compounds, although at different concentrations. Compound **16c** caused G2/M phase arrest and apoptosis at 0.3  $\mu$ M, while at least 1  $\mu$ M of the other inhibitors was needed to exert a comparable activity. Therefore, **16c** was the compound of choice for subsequent experiments.

### **Tubulin binding**

VDAs, including colchicine, arrest cell cycle progression at G2/M phase by interfering with tubulin polymerization. In order to evaluate whether our compounds bind to tubulin we carried out a recently described competition assay with *N,N'*-ethylene-bis(iodoacetamide) (EBI) in human breast cancer MDA-MB-231 cells.<sup>36</sup> EBI is an alkylating agent that specifically binds to two cysteine residues present in the colchicine-binding site of tubulin, Cys239 and Cys354. This  $\beta$ -tubulin adduct can be detected by western blot as a second immunoreactive  $\beta$ -tubulin band that migrates faster than  $\beta$ -tubulin itself. So, if EBI is added to cells previously treated with a colchicine-site binder, the binding site is already occupied and the EBI adduct cannot be observed. Since the distance between the different bands depends on the cell type, we used MDA-MB-231 cells in which the two bands can be easily distinguished. As shown in Figure 6, addition of EBI led to the appearance of a second band below the  $\beta$ -tubulin band. Addition of colchicine (**1**) (0.5  $\mu$ M) or **16c** (10  $\mu$ M) prevented the covalent binding of EBI in living MDA-MB-231 cells, resulting in the absence of the adduct band. This effect was also observed in the presence of the other compounds (data not shown). Thus, these data indicate that our compounds induce their anti-mitotic effects by binding to the colchicine-binding site in  $\beta$ -tubulin.

Binding of some representative inhibitors (**14c**, **16c** and **26f**) to tubulin was confirmed by competition with 2-methoxy-5-(2,3,4-trimethoxyphenyl)-2,4,6-cycloheptatrien-1-one (MTC) and (R)-(+)-ethyl 5-amino 2-methyl-1,2-dihydro-3-phenylpyrido[3,4-*b*]pyrazin-7-yl carbamate (R-PT), two well characterized, reversible colchicine-binding site ligands.<sup>37-40</sup> Indeed all three compounds displace both MTC and R-PT as determined by fluorescence spectroscopy (as shown in Fig. S3 for **16c** in the Supporting Information).

In order to determine their binding affinities, competition experiments with MTC, the lower affinity compound ( $K_a$   $4.7 \times 10^5$  M<sup>-1</sup>),<sup>41</sup> were performed. The data indicated a very high affinity making it difficult to precisely quantify the binding constant.<sup>42</sup> Therefore, the displacement of R-PT was used to measure the binding constants. First, we determined the binding constant of R-PT at 25° C ( $5.1 \times 10^6$  M<sup>-1</sup>) which was found to be 10 times higher than that of MTC, and similar to the previously reported value ( $3.2 \times 10^6$  M<sup>-1</sup>).<sup>43</sup> Then, R-PT displacement experiments were carried out with our three compounds allowing the determination of their binding affinities (Figure 7) in the sub-micromolar range (Table 2). Interestingly, the binding constants obtained are higher than those previously determined for other classical colchicine-binding site ligands, such as Nocodazole ( $4 \times 10^5$  M<sup>-1</sup>),<sup>44</sup> or Podofilotoxin ( $1.8 \times 10^6$  M<sup>-1</sup>).<sup>45</sup>

### **Inhibition of mitotic spindle formation.**

Next, we investigated whether the interaction of the compounds with tubulin affects the organization of tubulin into mitotic spindles during cell division.<sup>47</sup> Therefore, MDA-MB-231 cells were treated with colchicine (0.1 μM) or **16c** (1 μM) for 8 h after which the microtubules were visualized by immunofluorescence microscopy (Fig. 8). Whereas in the control cells (treated with 0.1% DMSO) chromosomes lined up along the metaphase plate and normal bipolar mitotic spindles extended from the cell poles toward the midpoint, highly aberrant, multipolar spindles were formed in the presence of colchicine or **16c**. Thus, the inability of the cells to proceed through the cell cycle after treatment with **16c** may be explained by the lack of DNA organization into a metaphase plate, which is required for proper cell division.

### **Anti-vascular Activity.**

Finally, we studied the capacity of this new family of anti-proliferative compounds to destroy a preexisting vasculature network formed by endothelial cells. HMEC-1 were seeded on top of matrigel, which induces their reorganization into tube-like structures within 3 h.<sup>34</sup> Then, colchicine (0.1-10 μM) or **16c** (0.1-10 μM)

were added. After 90 min of treatment the plates were photographed and the extent of tube formation was evaluated. As shown in Figure 9, colchicine displayed vascular disrupting effects at 0.1  $\mu$ M with total destruction of the cord-like structures at 0.3  $\mu$ M. Similar effects were observed in the presence of **16c**, but at 10-fold higher concentrations.

## Conclusions

Vascular disrupting agents show a great potential in cancer therapies and the limitations observed with those prototypes in clinical trials demand new chemical entities that could be useful as VDAs. Herein we describe the identification of a new family of anti-proliferative compounds with potential VDA-like properties.

Starting from a ligand 3-D shape similarity virtual screening approach using as queries compounds that target the  $\alpha,\beta$ -tubulin dimer at the colchicine-binding site, a cyclohexanedione derivative **9** was identified as a moderate cell growth inhibitor, both in tumor and endothelial cells. By performing a synthetic programme of structural analogues, structure-activity relationships could be established and six derivatives showed anti-proliferative activities in the sub-micromolar range, being 100-fold more potent than the initial hit, and only 10-fold less effective than colchicine itself, a well-known, but toxic, VDA. The compounds described herein inhibit endothelial and tumor cell proliferation at sub-micromolar concentrations, doses at which also their inhibitory effects on the cell cycle and endothelial morphology were observed. Binding at the colchicine site was confirmed by means of fluorescence measurements of MTC and R-PT displacement, and the binding constants obtained are in the  $\mu$ M range. Thus, these colchicine-binding compounds represent a very promising family of anti-proliferative and anti-vascular agents that are being further explored.

## Experimental section

### Computational methods.

All VS calculations have been performed in a Dell Precision T7400 workstation. The software used for the VS (FILTER, OMEGA, ROCS and VIDA) were obtained from OpenEye Scientific Software ([www.eyesopen.com](http://www.eyesopen.com)) by an academic license.

**Database preparation.** The database compounds were obtained from the ZINC database,<sup>19</sup> version 8 and contained about 8.5 million compounds in SMILE string format.<sup>20</sup> The initial filter was performed with the

“drug-like filter” implemented in the tool FILTER v2.1.1 and only selected terms were customized from the default file. The filtered dataset was thus reduced to 2.8 million compounds. 2D to 3D conversion and generation of conformational ensembles was carried out with OMEGA v2.3.2. This tool is controlled by a configuration file in which three parameters were changed as compared to the default values. The maximum number of output conformations of each molecule was set to 300; the energy window was set to 20 kcal/mol in order to discard high-energy conformations; and finally, a rmsd cut-off of 0.75 Å below which two conformations are considered to be the same. When the data set was then submitted to OMEGA, a total of 510 million chemical entities (in mol2 format) were obtained and submitted to the VS protocol.

**Virtual Screening with ROCS.** ROCS v3.1.2 (Rapid Overlay of Chemical Structures) method was used for the virtual screening. ROCS overlays the multiconformer compound’s database in shape and chemistry (“color”) with respect to the reference ligand. As query molecules, a single conformation found in the  $\alpha,\beta$ -tubulin-ligand X-Ray structures of DAMA-colchicine (pdb 1sa0)<sup>26</sup> and TN-16 (pdb 3hkd)<sup>27</sup> were used. ROCS was run using the default settings. The output conformations of ROCS were ranked according to their shape similarity with the query using a Tanimoto coefficient of 0.75 and a ComboScore (shape plus color) of 1.4. Final results were visualized and analyzed with VIDA v4.1.1. VS carried out with TN-16 as query, resulted in a total of 170 compounds, that were clustered by visual inspection into 9 chemical families. Only the best ranked compound of each family was selected as hit for the antiproliferative assay, of which, only six were available at the time and subsequently tested.

## Chemistry procedures

Melting points were obtained on a Reichert-Jung Kofler apparatus and are uncorrected. The elemental analysis was performed with a Heraeus CHN-O-RAPID instrument. The elemental compositions of the compounds agreed to within  $\pm 0.4\%$  of the calculated values. For all the tested compounds, satisfactory elemental analysis was obtained supporting  $>95\%$  purity. Electrospray mass spectra were measured on a quadrupole mass spectrometer equipped with an electrospray source (Hewlett-Packard, LC/MS HP 1100).  $^1\text{H}$  and  $^{13}\text{C}$  NMR spectra were recorded on a Varian INNOVA 300 operating at 299 MHz ( $^1\text{H}$ ) and 75 MHz ( $^{13}\text{C}$ ), respectively, a Varian INNOVA-400 operating at 399 MHz ( $^1\text{H}$ ) and 99 MHz ( $^{13}\text{C}$ ), respectively, and a VARIAN SYSTEM-500 operating at 499 MHz ( $^1\text{H}$ ) and 125 MHz ( $^{13}\text{C}$ ), respectively.

Analytical TLC was performed on silica gel 60 F<sub>254</sub> (Merck) precoated plates (0.2 mm). Spots were detected under UV light (254 nm) and/or charring with ninhydrin or phosphomolibdic acid. Separations on silica gel were performed by preparative centrifugal circular thin-layer chromatography (CCTLC) on a Chromatotron<sup>R</sup> (Kiesegel 60 PF<sub>254</sub> gipshaltig (Merck)), with layer thickness of 1 and 2 mm and flow rate of 4 or 8 mL/min, respectively. Flash column chromatography was performed in a Biotage Horizon instrument.

Microwave reactions were performed using the Biotage Initiator 2.0 single-mode cavity instrument from Biotage (Uppsala). Experiments were carried out in sealed microwave process vials utilizing the standard absorbance level (400 W maximum power). The temperature was measured with an IR sensor on the outside of the reaction vessel.

The synthesis of the different series of compounds has been performed applying the here described general procedures. A few key compounds are described in this Experimental section. Still full details and analytical and spectroscopic data for all the compounds are included in the Supporting Information.

#### **5-oxo-1,2,5,6-tetrahydro-[1,1'-biphenyl]-3-yl propionate (**11**).**

To a solution of 5-phenylcyclohexane-1,3-dione (300 mg, 1.59 mmol) and DMAP (59 mg, 0.48 mmol) in CH<sub>2</sub>Cl<sub>2</sub> (1.6 mL), Hunig's base (DIPEA) (277  $\mu$ L, 1.59 mmol) was added. Then, propionyl chloride (147  $\mu$ L, 1.59) was added dropwise and the reaction mixture was refluxed for 2 h. After cooling, HCl 1N (10 mL) was added and the crude extracted with ethyl acetate (10 mL x 3). The organic layer was washed with brine (15 mL), dried over Na<sub>2</sub>SO<sub>4</sub>, concentrated, and purified by flash chromatography (hexane/ethyl acetate 3:1) to yield 250 mg (64 %) of **11** as an oil. EM (ES, positive mode): *m/z* 245 (M+H)<sup>+</sup>. <sup>1</sup>H NMR (DMSO-d<sub>6</sub>, 300 MHz)  $\delta$ : 1.07 (t, 3H, *J* = 7.4 Hz, CH<sub>3</sub>), 2.57 (s, 3H, CH<sub>3</sub>), 2.66 (m, 2H, H-4, H-6), 2.81 (m, 2H, H-4, H-6), 3.28 (m, 1H, H-5), 5.91 (d, 1H, *J* = 2.1 Hz, H-2), 7.24 (m, 1H, Ar), 7.35 (m, 4H, Ar).

#### **5-Phenyl-2-propionylcyclohexane-1,3-dione (**12**).**

A microwave vial was charged with 5-phenylcyclohexane-1,3-dione (**10**) (500 mg, 2.66 mmol), propionyl chloride (490  $\mu$ L, 5.31 mmol), anhydrous K<sub>2</sub>CO<sub>3</sub> (809 mg, 5.85 mmol), 1,2,4-triazole (73 mg, 1.06 mmol) and tetrabutylammonium bromide (429 mg, 1.33 mmol) in anhydrous acetonitrile (10 mL). The reaction vessel was sealed, stirred under argon atmosphere for 10 minutes and heated in a microwave reactor at 70 °C for 2 h. After cooling, the reaction mixture was acidified with 1N HCl and the mixture was extracted with ethyl acetate. The organic layer was dried over Na<sub>2</sub>SO<sub>4</sub>, concentrated, and purified by flash chromatography (hexane/ethyl acetate) to yield 330 mg (51%) of **12** as a white solid. Mp 71-73 °C. EM (ES, positive mode):

m/z 245 (M+H)<sup>+</sup>. <sup>1</sup>H NMR (DMSO-d<sub>6</sub>, 300 MHz) δ (enol form): 1.05 (t, 3H, *J* = 7.3 Hz, CH<sub>3</sub>), 2.62-2.71 (m, 2H, H-4, H-6), 2.87-2.95 (m, 2H, H-4, H-6), 3.01 (q, 2H, *J* = 7.2 Hz, CH<sub>2</sub>), 3.46 (m, 1H, H-5), 7.23-7.38 (m, 5H, Ar). Although this compound was mentioned in ref 28 no analytical or spectroscopic data were provided.

#### **General procedure for the reaction of 2-acyl-5-phenylcyclohexane-1,3-diones with anilines**

A microwave vial was charged with 2-acyl-5-phenylcyclohexane-1,3-dione (1.0 mmol), the appropriate aniline (1.5 mmol) and 4 Å molecular sieves in toluene (2 mL). The reaction vessel was sealed and heated in a microwave reactor at 150 °C for 2 h. After cooling, the solvent was evaporated. The resulting residue was purified as specified.

#### **2-(1-((3-Hydroxyphenyl)amino)propylidene)-5-phenylcyclohexane-1,3-dione (14a).**

Following the general procedure for the reaction of 2-acyl-5-phenylcyclohexane-1,3-diones with anilines, a microwave vial was charged with 5-phenyl-2-propionylcyclohexane-1,3-dione (**12**) (40 mg, 0.16 mmol) and 3-aminophenol (26 mg, 0.24 mmol) in toluene. The residue was worked up and purified by CCTLC in the Chromatotron (dichloromethane/methanol, 40:1) to yield 50 mg (93%) of **14a** as a white solid. Mp 199-201 °C. EM (ES, positive mode): m/z 336 (M+H)<sup>+</sup>. <sup>1</sup>H NMR (DMSO-d<sub>6</sub>, 500 MHz) δ: 1.06 (t, 3H, *J* = 7.3 Hz, CH<sub>3</sub>), 2.60-2.64 (m, 2H, H-4, H-6), 2.80-2.89 (m, 4H, H-4, H-6, CH<sub>2</sub>), 3.33 (m, 1H, H-5), 6.65 (t, 1H, *J* = 2.2 Hz, Ar), 6.70 (m, 1H, Ar), 6.81 (ddd, 1H, *J* = 8.2, 2.4, 0.9 Hz, Ar), 7.18-7.25 (m, 1H, Ar), 7.27 (t, 1H *J* = 8.0 Hz, Ar), 7.32 (d, 4H, *J* = 4.4 Hz, Ar), 9.90 (br s, 1H, OH), 14.94 (br s, 1H, NH). <sup>13</sup>C NMR (DMSO-d<sub>6</sub>, 125 MHz) δ: 12.8 (CH<sub>3</sub>), 23.4 (CH<sub>2</sub>), 36.0 (C-5), 46.0 (C-4, C-6), 106.7 (NHC=C), 112.9, 115.8, 116.4, 126.5, 126.7, 128.5, 130.4, 136.8, 143.4, 158.2 (Ar), 177.0 (NHC=C). Anal. calc. for (C<sub>21</sub>H<sub>21</sub>NO<sub>3</sub>): C, 75.20; H, 6.31; N, 4.18. Found: C, 75.33; H, 6.12; N, 4.36.

#### **2-(1-((4-Hydroxyphenyl)amino)propylidene)-5-phenylcyclohexane-1,3-dione (14b).**

Following the general procedure for the reaction of 2-acyl-5-phenylcyclohexane-1,3-diones with anilines, a microwave vial was charged with 5-phenyl-2-propionylcyclohexane-1,3-dione (**12**) (40 mg, 0.16 mmol) and 4-aminophenol (26 mg, 0.24 mmol) in toluene. The residue was worked up and purified by CCTLC in the Chromatotron (dichloromethane/methanol 40:1) to yield 30 mg (56%) of **14b** as a white solid. Mp 203-205 °C. EM (ES, positive mode): m/z 336 (M+H)<sup>+</sup>. <sup>1</sup>H NMR (DMSO-d<sub>6</sub>, 300 MHz) δ: 1.02 (t, 3H, *J* = 7.3 Hz, CH<sub>3</sub>), 2.59-2.63 (m, 2H, H-4, H-6), 2.78-2.88 (m, 4H, H-4, H-6, CH<sub>2</sub>), 3.32 (m, 1H, H-5), 6.85 (m, 2H, Ar), 7.11 (m, 2H, Ar), 7.23 (m, 1H, Ar), 7.33 (d, 4H, *J* = 4.4 Hz, Ar), 9.81 (br s, 1H, OH), 14.73 (br s, 1H, NH). <sup>13</sup>C NMR (DMSO d<sub>6</sub>, 100 MHz) δ: 13.0 (CH<sub>3</sub>), 23.7 (CH<sub>2</sub>), 36.5 (C-5), 46.5 (C-4, C-6), 107.1 (NHC=C),



116.4, 127.0, 127.2, 127.3, 127.7, 128.9, 143.9, 157.5 (Ar), 178.0 (NHC=C). Anal. calc. for (C<sub>21</sub>H<sub>21</sub>NO<sub>3</sub>): C, 75.20; H, 6.31; N, 4.18. Found: C, 74.98; H, 6.13; N, 4.37.

#### **2-(1-((2-Methoxyphenyl)amino)propylidene)-5-phenylcyclohexane-1,3-dione (14c).**

Following the general procedure for the reaction of 2-acyl-5-phenylcyclohexane-1,3-diones with anilines, a microwave vial was charged with 5-phenyl-2-propionylcyclohexane-1,3-dione (**12**) (35 mg, 0.14 mmol) and *o*-anisidine (24  $\mu$ L, 0.21 mmol) in toluene. The residue was worked up and purified by CCTLC in the Chromatotron (hexane/ethyl acetate, 5:1) to yield 48 mg (98%) of **14c** as a white solid. Mp 93-95 °C. EM (ES, positive mode):  $m/z$  350 (M+H)<sup>+</sup>. <sup>1</sup>H NMR (DMSO-d<sub>6</sub>, 400 MHz)  $\delta$ : 0.98 (t, 3H,  $J$  = 7.3 Hz, CH<sub>3</sub>), 2.59-2.64 (m, 2H, H-4, H-6), 2.80-2.84 (m, 4H, H-4, H-6, CH<sub>2</sub>), 3.36 (m, 1H, H-5), 3.82 (s, 3H, OCH<sub>3</sub>), 7.06 (td, 1H,  $J$  = 7.6, 1.2 Hz, Ar), 7.19-7.27 (m, 2H, Ar), 7.30 (dd, 1H,  $J$  = 7.7, 1.5 Hz, Ar), 7.33 (d, 2H,  $J$  = 1.4 Hz, Ar), 7.34 (s, 2H, Ar), 7.39-7.46 (m, 1H, Ar), 14.69 (br s, 1H, NH). <sup>13</sup>C NMR (DMSO-d<sub>6</sub>, 100 MHz)  $\delta$ : 12.2 (CH<sub>3</sub>), 25.5 (CH<sub>2</sub>), 36.0 (C-5), 46.1 (C-4, C-6), 55.8 (OCH<sub>3</sub>), 106.9 (NHC=C), 112.4, 120.7, 124.2, 126.5, 126.7, 127.5, 128.5, 129.7, 143.5, 153.5 (Ar), 178.0 (NHC=C). Anal. calc. for (C<sub>22</sub>H<sub>23</sub>NO<sub>3</sub>): C, 75.62; H, 6.63; N, 4.01. Found: C, 75.48; H, 6.52; N, 4.00.

Details of the synthesis and analytical and spectroscopic data for compounds **14d-j** are provided in the Supporting Information.

#### **2-Butyryl-5-phenylcyclohexane-1,3-dione (15a)**

Following the described procedure for the synthesis of **12**, a microwave vial was charged with 5-phenylcyclohexane-1,3-dione (**10**) (500 mg, 2.66 mmol), butyrylchloride (548  $\mu$ L, 5.31 mmol), anhydrous K<sub>2</sub>CO<sub>3</sub> (809 mg, 5.85 mmol), 1,2,4-triazole (73 mg, 1.06 mmol) and tetrabutylammonium bromide (429 mg, 1.33 mmol) in anhydrous acetonitrile (10 mL) to yield 200 mg (29%) of **15a** as a white solid. Mp 68-70 °C. EM (ES, positive mode):  $m/z$  259 (M+H)<sup>+</sup>. <sup>1</sup>H NMR (DMSO-d<sub>6</sub>, 300 MHz)  $\delta$  (enol form): 0.92 (t, 3H,  $J$  = 7.3 Hz, CH<sub>3</sub>), 1.58 (m, 2H, CH<sub>2</sub>), 2.69 (m, 2H, H-4, H-6), 2.92 (m, 2H, H-4, H-6), 2.97 (t, 2H,  $J$  = 7.4 Hz, CH<sub>2</sub>), 3.37-3.45 (m, 1H, H-5), 7.25 (m, 1H Ar), 7.33 (m, 4H, Ar). Note: Although this compound was mentioned in ref 29, no analytical data were provided.

#### **2-Acetyl-5-phenylcyclohexane-1,3-dione (15b).**

Following the described procedure for the synthesis of **12**, a microwave vial was charged with 5-phenylcyclohexane-1,3-dione (**10**) (500 mg, 2.66 mmol), acetylchloride (417  $\mu$ L, 5.31 mmol), anhydrous K<sub>2</sub>CO<sub>3</sub> (809 mg, 5.85 mmol), 1,2,4-triazole (73 mg, 1.06 mmol) and tetrabutylammonium bromide (429 mg,

1.33 mmol) in anhydrous acetonitrile (10 mL) to yield 350 mg (54%) of **15b** as a white solid. Mp 100-102 °C. EM (ES, positive mode):  $m/z$  231 ( $M+H$ )<sup>+</sup>. <sup>1</sup>H NMR (DMSO-*d*<sub>6</sub>, 300 MHz)  $\delta$  (enol form): 2.55 (s, 3H, CH<sub>3</sub>), 2.66-2.72 (m, 2H, H-4, H-6), 2.94 (m, 2H, H-4, H-6), 3.36-3.47 (m, 1H, H-5), 7.22-7.34 (m, 5H, Ar). Note: Although this compound was mentioned in ref 29, no analytical data were provided.

#### **2-((2-Methoxyphenyl)amino)butylidene)-5-phenylcyclohexane-1,3-dione (16a).**

A mixture of 2-butyryl-5-phenylcyclohexane-1,3-dione (**15a**) (60 mg, 0.23 mmol) and *o*-anisidine (30  $\mu$ L, 0.22 mmol) in 1.5 mL of toluene was heated for two days under reflux in a flask equipped with a Dean-Stark trap. Volatiles were removed and the crude reaction mixture was purified by CCTLC in the Chromatotron (hexane/ethyl acetate, 5:1) to yield 70 mg (84%) of **16a** as a pale yellow solid. Mp 108-110 °C. EM (ES, positive mode):  $m/z$  364 ( $M+H$ )<sup>+</sup>. <sup>1</sup>H NMR (DMSO-*d*<sub>6</sub>, 400 MHz)  $\delta$ : 0.74 (t, 3H,  $J$  = 7.3 Hz, CH<sub>3</sub>), 1.40 (m, 2H, CH<sub>2</sub>), 2.59-2.63 (m, 2H, H-4, H-6), 2.77 (m, 4H, H-4, H-6, CH<sub>2</sub>), 3.29-3.37 (m, 1H, H-5), 3.82 (s, 3H, OCH<sub>3</sub>), 7.05 (m, 1H,  $J$  = 7.6, 1.2 Hz, Ar), 7.21 (dd, 1H,  $J$  = 8.4, 1.2 Hz, Ar), 7.25 (m, 1H, Ar), 7.28 (dd, 1H,  $J$  = 7.7, 1.6 Hz, Ar), 7.33 (d, 2H,  $J$  = 1.3 Hz, Ar), 7.33 (s, 2H, Ar), 7.42 (ddd, 1H,  $J$  = 8.6, 7.6, 1.6 Hz, Ar), 14.73 (br s, 1H, NH). <sup>13</sup>C NMR (DMSO-*d*<sub>6</sub>, 100 MHz)  $\delta$ : 14.1 (CH<sub>3</sub>), 21.3 (CH<sub>2</sub>), 31.9 (CH<sub>2</sub>), 36.0 (C-5), 46.0, 46.5 (C-4, C-6), 55.8 (OCH<sub>3</sub>), 107.2 (NHC=C), 112.3, 120.7, 124.4, 126.5, 126.5, 127.5, 128.5, 129.6, 143.4, 153.5 (Ar), 176.4 (NHC=C). Anal. calc. for (C<sub>23</sub>H<sub>25</sub>NO<sub>3</sub>): C, 76.01; H, 6.93; N, 3.85. Found: C, 75.93; H, 6.68; N, 4.10.

#### **5-Phenyl-2-(1-(*o*-tolylamino)butylidene)cyclohexane-1,3-dione (16b).**

Following the general procedure for the reaction of 2-acyl-5-phenylcyclohexane-1,3-diones with anilines, a microwave vial was charged with 2-butyryl-5-phenylcyclohexane-1,3-dione (**15a**) (30 mg, 0.12 mmol) and *o*-toluidine (18  $\mu$ L, 0.17 mmol) in toluene. The residue was worked up and purified by CCTLC in the Chromatotron (hexane/ethyl acetate, 5:1) to yield 42 mg (99%) of **16b** as a white solid. Mp 98-100 °C. EM (ES, positive mode):  $m/z$  348 ( $M+H$ )<sup>+</sup>. <sup>1</sup>H NMR (DMSO-*d*<sub>6</sub>, 500 MHz)  $\delta$ : 0.74 (t, 3H,  $J$  = 7.3 Hz, CH<sub>3</sub>), 1.40 (m, 2H, CH<sub>2</sub>), 2.17 (s, 3H, CH<sub>3</sub>), 2.63 (dd, 2H,  $J$  = 16.7, 3.7 Hz, H-4, H-6), 2.75 (t, 2H,  $J$  = 7.3 Hz, CH<sub>2</sub>), 2.85 (m, 2H, H-4, H-6), 3.32-3.39 (m, 1H, H-5), 7.22-7.26 (m, 1H, Ar), 7.27 (dd, 1H,  $J$  = 7.2, 2.1 Hz, Ar), 7.34 (m, 6H, Ar), 7.41 (m, 1H, Ar), 14.91 (br s, 1H, NH). <sup>13</sup>C NMR (DMSO-*d*<sub>6</sub>, 125 MHz)  $\delta$ : 14.2 (CH<sub>3</sub>), 17.5 (CH<sub>3</sub>), 21.3 (CH<sub>2</sub>), 31.8 (CH<sub>2</sub>), 36.0 (C-5), 46.0 (C-4, C-6), 107.0 (NHC=C), 126.5, 126.7, 126.8, 126.9, 128.3, 128.5, 131.0, 133.6, 135.0, 143.5 (Ar), 176.1 (NHC=C). Anal. calc. for (C<sub>23</sub>H<sub>25</sub>NO<sub>2</sub>): C, 79.51; H, 7.25; N, 4.03. Found: C, 79.27; H, 6.98; N, 4.11.

### **2-(1-((2-Methoxyphenyl)amino)ethylidene)-5-phenylcyclohexane-1,3-dione (16c).**

Following the general procedure for the reaction of 2-acyl-5-phenylcyclohexane-1,3-diones with anilines, a microwave vial was charged with 2-acetyl-5-phenylcyclohexane-1,3-dione (**15b**) (40 mg, 0.17 mmol) and *o*-anisidine (30  $\mu$ L, 0.26 mmol) in toluene. The residue was worked up and purified by CCTLC in the Chromatotron (hexane/ ethyl acetate, 5:1) to yield 49 mg (86%) of **16c** as a white solid. Mp 139-141 °C. EM (ES, positive mode):  $m/z$  336 (M+H)<sup>+</sup>. <sup>1</sup>H NMR (DMSO-d<sub>6</sub>, 500 MHz)  $\delta$ : 2.41 (s, 3H, CH<sub>3</sub>), 2.60-2.63 (m, 2H, H-4, H-6), 2.82 (m, 2H, H-4, H-6), 3.36 (m, 1H, H-5), 3.84 (s, 3H, OCH<sub>3</sub>), 7.04 (td, 1H,  $J$  = 7.6, 1.2 Hz, Ar), 7.20 (dd, 1 H,  $J$  = 8.5, 1.2 Hz, Ar), 7.21–7.26 (m, 1H, Ar), 7.32 (dd, 1H,  $J$  = 7.8, 1.6 Hz, Ar), 7.33 (d, 2H,  $J$  = 0.8 Hz, Ar), 7.34 (s, 2H, Ar), 7.39 (m, 1H, Ar), 14.78 (br s, 1H, NH). <sup>13</sup>C NMR (DMSO-d<sub>6</sub>, 125 MHz)  $\delta$ : 19.7 (CH<sub>3</sub>), 36.1 (C-5), 46.4 (C-4, C-6), 55.8 (OCH<sub>3</sub>), 108.4 (NHC=C), 112.3, 120.6, 124.5, 126.5, 126.7, 128.9, 128.5, 129.2, 143.5, 153.1 (Ar), 172.4 (NHC=C). Anal. calc. for (C<sub>21</sub>H<sub>21</sub>NO<sub>3</sub>): C, 75.20; H, 6.31; N, 4.31. Found: C, 74.98; H, 6.32; N, 4.20.

### **5-Phenyl-2-(1-(*o*-tolylamino)ethylidene)cyclohexane-1,3-dione (16d).**

Following the general procedure for the reaction of 2-acyl-5-phenylcyclohexane-1,3-diones with anilines, a microwave vial was charged with 2-acetyl-5-phenylcyclohexane-1,3-dione (**15b**) (30 mg, 0.13 mmol) and *o*-toluidine (22  $\mu$ L, 0.20 mmol) in toluene. The residue was worked up and purified by CCTLC in the Chromatotron (hexane/ethyl acetate, 5:1) to yield 25 mg (60%) of **16d** as a white solid. Mp 128-130 °C. EM (ES, positive mode):  $m/z$  320 (M+H)<sup>+</sup>. <sup>1</sup>H NMR (DMSO-d<sub>6</sub>, 300 MHz)  $\delta$ : 2.20 (s, 3H, CH<sub>3</sub>), 2.38 (s, 3H, CH<sub>3</sub>), 2.59-2.66 (m, 2H, H-4, H-6), 2.79-2.89 (m, 2H, H-4, H-6), 3.36 (m, 1H, H-5), 7.23-7.40 (m, 9H, Ar), 14.91 (br s, 1H, NH). <sup>13</sup>C NMR (DMSO-d<sub>6</sub>, 100 MHz)  $\delta$ : 17.4 (CH<sub>3</sub>), 19.6 (CH<sub>3</sub>), 36.1 (C-5), 45.8 (C-4, C-6), 108.2 (NHC=C), 126.5, 126.7, 126.9, 128.1, 128.49, 131.0, 133.3, 135.1, 143.5, 159.9 (Ar), 172.7 (NHC=C). Anal. calc. for (C<sub>21</sub>H<sub>21</sub>NO<sub>2</sub>): C, 78.97; H, 6.63; N, 4.39. Found: C, 78.69; H, 6.54; N, 4.27.

## **Biological methods**

### **Cell proliferation.**

Endothelial cells. Mouse brain endothelial cells (MBEC), bovine aortic endothelial cells (BAEC) and human dermal microvascular endothelial cells (HMEC-1) were seeded in 48-well plates at 10,000 cells/well (except HMEC-1 at 20,000/well). After 24 h, 5-fold dilutions of the compounds were added. The cells were allowed to proliferate 3 days (or 4 days for HMEC-1) in the presence of the compounds, trypsinized, and counted by means of a Coulter counter (Analys, Belgium).

**Tumor cells.** Human cervical carcinoma (HeLa) cells were seeded in 96-well plates at 15,000 cells/well in the presence of different concentrations of the compounds. After 4 days of incubation, the cells were trypsinized and counted in a Coulter counter. Suspension cells (Mouse leukemia L1210 and human lymphoid Cem cells) were seeded in 96-well plates at 60,000 cells/well in the presence of different concentrations of the compounds. L1210 and Cem cells were allowed to proliferate for 48 h or 96 h, respectively and then counted in a Coulter counter. The 50% inhibitory concentration ( $IC_{50}$ ) was defined as the compound concentration required to reduce cell proliferation by 50%. Colchicine was added as reference compound.

**Cell cycle analysis.** HMEC-1 cells were seeded in 6-well plates at 125,000 cells/well in DMEM with 10 % FCS. After 24 h, the cells were exposed to different concentrations of the compounds. After 24 h, the DNA of the cells was stained with propidium iodide using the CycleTEST PLUS DNA Reagent Kit (BD Biosciences, San Jose, CA). The DNA content of the stained cells was assessed by flow cytometry on a FACSCalibur flow cytometer and analyzed with CellQuest software (BD Biosciences) within 3h after staining. Cell debris and clumps were excluded from the analysis by appropriate dot plot gating. Percentages of sub-G1, G1, S, and G<sub>2</sub>/M cells were estimated using appropriate region markers.<sup>35</sup> Colchicine was added as reference compound.

**Tube formation.** Wells of a 96-well plate were coated with 70  $\mu$ l matrigel (10 mg/ml, BD Biosciences, Heidelberg, Germany) at 4°C. After gelatinization at 37°C during 30 min, HMEC-1 cells were seeded at 60,000 cells/well on top of the matrigel in 200  $\mu$ l DMEM containing 10% FCS. After 3 h of incubation at 37°C, when the endothelial cells had reorganized to form tube-like structures, the compounds were added. Ninety minutes later, colchicine, which was added as a reference compound, had destroyed the endothelial tubes. The cultures were photographed at 100 x magnification.

**Tubulin binding.** Human breast carcinoma MDA-MB-231 cells were seeded in 6-well plates at 500,000 cells/well. After 48 h, compounds were added to the cells for 16 h before adding EBI (N,N'-ethylene-bis(iodoacetamide) at 100  $\mu$ M. After 1.5 h, the cells were harvested and cell extracts were prepared for western blot analysis. Twenty  $\mu$ g of proteins were subjected to gel electrophoresis using 0.1% SDS (85% purity) and 10% polyacrylamide gels. After electrophoresis, proteins were transferred to pretreated Hybond-P polyvinylidene difluoride (PVDF) membranes (Amersham Biosciences). The membranes were incubated for 1 h at room temperature in blocking buffer (2.5 % non-fat dry milk in PBS containing 0.1% Tween) and subsequently for 16 h at 4°C in blocking buffer with primary antibodies raised against  $\beta$ -tubulin. After washing, the membranes were incubated with the corresponding horseradish peroxidase-conjugated

secondary antibody in blocking buffer for 25 min at room temperature. Next, the membranes were washed extensively. Immunoreactive proteins were detected by chemiluminescence (ECLplus, Bio-Rad).

In living cells, EBI cross-links the cysteine residues at positions 239 and 354 of  $\beta$ -tubulin. This  $\beta$ -tubulin adduct formed by EBI is easily detectable by western blot as a second immunoreactive band that migrates faster than  $\beta$ -tubulin. Colchicine was added as a reference compound.

#### **Determination of binding constants.**

Proteins and ligands. Calf brain tubulin was purified as described.<sup>48</sup> 2-methoxy-5-(2,3,4-trimethoxyphenyl)-2,4,6-cycloheptatrien-1-one (MTC)<sup>49</sup> was a kind gift of Prof. T.J. Fitzgerald School of Pharmacy, Florida A & M University. (R)-(+)-ethyl 5-amino 2-methyl-1,2-dihydro-3-phenylpyrido[3,4-b]pyrazin-7-yl carbamate (R-PT) [ENREF 53](#)<sup>50</sup> was a kind gift of Prof. G.A. Rener, Organic Chemistry Research Department, Southern Research Institute, Birmingham, Alabama. The compounds were diluted in 99.8% D6-DMSO (Merck, Darmstadt, Germany) to a final concentration of 10 mM and stored at -80 °C.

Determination of binding constants. Competition of the compounds with MTC was tested by the change in the intensity of fluorescence of MTC upon binding to tubulin. The fluorescence emission spectra (excitation at 350 nm) of 10  $\mu$ M Tubulin and 10  $\mu$ M MTC in 10 mM Sodium Phosphate, 0.1 mM GTP pH 7.0 were measured in the presence or the absence of 20  $\mu$ M of the desired ligand with 5 nm excitation and emission slits using a Jobin-Yvon SPEX Fluoromax-2 (HORIBA, Ltd. Kyoto, Japan). The decrease in the intensity of the fluorescence in the presence of the competitor ligand indicated competition for the same binding site.

The binding constant of R-PT for dimeric tubulin was determined using the competition method in 10 mM sodium phosphate, 0.1 mM GTP pH 7.0 at 25°C. To do so 0.2  $\mu$ M of R-PT was incubated with increasing amounts of tubulin up to 10 $\mu$ M and vice versa, 0.2  $\mu$ M of tubulin was incubated with increasing amounts of R-PT up to 10 $\mu$ M, the fluorescence emission spectra (excitation 374 nm) of the samples (5 nm excitation and emission slits) were determined using a Jobin-Yvon SPEX Fluoromax-2 (HORIBA, Ltd. Kyoto, Japan). Using these spectra it is possible to calculate the free and the bound R-PT concentration for each sample and thus to determine the binding constant of R-PT for tubulin.

Once  $K_b$  of R-PT is determined ( $5.1 \times 10^6 \text{ M}^{-1}$ ) this compound could be used as a reference ligand as described in .For that purpose, the fluorescence emission of a previous mixed sample of 0.2 $\mu$ M of R-PT and 0.2  $\mu$ M of tubulin was evaluated in the presence of increasing concentrations of studied ligand in a black 96-well plate (0; 0.05; 0.2; 0.5; 2; 5; 10; 30; 50; 70  $\mu$ M). The samples were incubated 30 minutes at 25°C in a

*Varioskan* plate reader (Thermo Scientific Waltham, Massachusetts, USA) before the fluorescence emission intensity at 456 nm (excitation 374 nm) was measured. The data were analyzed and the binding constants determined using Equigra V5.0.<sup>42</sup>

**Immunocytochemistry.** MDA-MB-231 cells were grown on poly-L-Lysine pre-coated 8-well chamber slides (Lab-Tek, Nunc, Roskilde, Denmark) in DMEM containing 10% FBS and exposed to compound (DMSO, **16c** or colchicine). After 8 h, the cells were fixed in 4% PFA for 15 min at room temperature, washed three times with PBS and permeabilized for 10 min at room temperature with 0.25% Triton X-100 (Sigma-Aldrich). Nonspecific binding sites were blocked for 30 min at room temperature with 0.5% BSA in PBS. The cells were then incubated with a monoclonal anti- $\beta$ -tubulin antibody (2  $\mu$ g/ml, Sigma-Aldrich) for 2 h at room temperature, washed three times and incubated for 1 h at room temperature with goat anti-mouse Alexa Fluor 488 (4  $\mu$ g/ml; Molecular Probes, Invitrogen) in 0.5% BSA. After three washes, nuclei were stained with 300 nM 4',6-diamidino-2-phenylindole (DAPI; Sigma-Aldrich). Fluorescent microscopic analysis was done with anAxiovert 200 M inverted microscope (Zeiss, Göttingen, Germany), using an EC Plan-Neofluar 40x/1.30 oil objective. Pictures were taken with an AxioCamMRm camera and processed with AxioVision Release 4.6 software (Zeiss).

### **Acknowledgments.**

M.-D. C. thanks the Fondo Social Europeo (FSE) and the JAE Predoc Programme for a predoctoral fellowship. This work has received the ALMIRALL S.A award for young researchers (to M.-D. C) in the XVI call sponsored by the Spanish Society of Medicinal Chemistry (SEQT). This project has been supported by the Spanish Plan Nacional (SAF2009-13914-C02-01 and SAF2012-39760-C02-01 to MJC), Comunidad de Madrid (BIPEDD2; ref. P2010/BMD-2457 to MJC and JFD), the BIO2010-16351 (to JFD) project from the

Ministry of Economy and Competitiveness of Spain, and a FPI grant to Gonzalo Sáez-Calvo. We also wish to thank Eef Meyen and Lizette van Berckelaer for excellent technical assistance. We are indebted to Matadero Vicente de Lucas de Segovia for providing calf brains for the tubulin purification.

SUPPORTING INFORMATION AVAILABLE. The synthesis and spectroscopic data of all the synthesized compounds is included. Molecular structures (SMILES strings) of the virtual screening hits tested are included in Table S1. Anti-proliferative activity of the VS hits in endothelial and tumor cell lines is included in Table S2. Dose-response curves of **9** in endothelial and tumor cell lines is included as Figure S2. Fluorescence emission spectra for the displacement of MTC by **9** and R-PT and MTC by **16c** are included as Figures S1 and S3, respectively. This material is available free of charge via the Internet at <http://pubs.acs.org>

## References.

1. Folkman, J.; Bach, M.; Rowe, J. W.; Davidoff, F.; Lambert, P.; Hirsch, C.; Goldberg, A.; Hiatt, H. H.; Glass, J.; Henshaw, E. Tumor angiogenesis - Therapeutic implications. *N. Engl. J. Med.* **1971**, *285*, 1182-1186.
2. (a) Roodink, I.; Leenders, W. P. J. Targeted therapies of cancer Angiogenesis inhibition seems not enough. *Cancer Lett.* **2010**, *299*, 1-10; (b) Siemann, D. W.; Bibby, M. C.; Dark, G. G.; Dicker, A. P.; Eskens, F.; Horsman, M. R.; Marme, D.; LoRusso, P. M. Differentiation and definition of vascular-targeted therapies. *Clin. Cancer Res.* **2005**, *11*, 416-420.
3. Potente, M.; Gerhardt, H.; Carmeliet, P. Basic and Therapeutic Aspects of Angiogenesis. *Cell* **2011**, *146*, 873-887.
4. McKeage, M. J.; Baguley, B. C. Disrupting Established Tumor Blood Vessels An Emerging Therapeutic Strategy for Cancer. *Cancer* **2010**, *116*, 1859-1871.
5. Mita, M. M.; Sargsyan, L.; Mita, A. C.; Spear, M. Vascular-disrupting agents in oncology. *Expert. Opin. Invest. Drugs* **2013**, *22*, 317-328.
6. Denekamp, J. Endothelial cell proliferation as a novel approach to targeting tumor therapy. *Br. J. Cancer* **1982**, *45*, 136-139.
7. Siemann, D. W. The unique characteristics of tumor vasculature and preclinical evidence for its selective disruption by Tumor-Vascular Disrupting Agents. *Cancer Treat. Rev.* **2011**, *37*, 63-74.
8. (a) Konerding, M. A.; Fait, E.; Gaumann, A. 3D microvascular architecture of pre-cancerous lesions and invasive carcinomas of the colon. *Br. J. Cancer* **2001**, *84*, 1354-1362; (b) Kakolyris, S.; Fox, S. B.; Koukourakis, M.; Giatromanolaki, A.; Brown, N.; Leek, R. D.; Taylor, M.; Leigh, I. M.; Gatter, K. C.; Harris, A. L. Relationship of vascular maturation in breast cancer blood vessels to vascular density and

- metastasis, assessed by expression of a novel basement membrane component, LH39. *Br. J. Cancer* **2000**, *82*, 844-851.
9. Spear, M. A.; LoRusso, P.; Mita, A.; Mita, M. Vascular Disrupting Agents (VDA) in Oncology: Advancing Towards New Therapeutic Paradigms in the Clinic. *Curr. Drug Targets* **2011**, *12*, 2009-2015.
  10. Lu, Y.; Chen, J.; Xiao, M.; Li, W.; Miller, D. D. An Overview of Tubulin Inhibitors That Interact with the Colchicine Binding Site. *Pharm. Res.* **2012**, *29*, 2943-2971.
  11. Galbraith, S. M.; Chaplin, D. J.; Lee, F.; Stratford, M. R. L.; Locke, R. J.; Vojnovic, B.; Tozer, G. M. Effects of combretastatin A4 phosphate on endothelial cell morphology in vitro and relationship to tumour vascular targeting activity in vivo. *Anticancer Res.* **2001**, *21*, 93-102.
  12. Tozer, G. M.; Kanthou, C.; Baguley, B. C. Disrupting tumour blood vessels. *Nature Rev. Cancer* **2005**, *5*, 423-435.
  13. (a) Kanthou, C.; Tozer, G. M. The tumor vascular targeting agent combretastatin A-4-phosphate induces reorganization of the actin cytoskeleton and early membrane blebbing in human endothelial cells. *Blood* **2002**, *99*, 2060-2069; (b) Davis, P. D.; Dougherty, G. J.; Blakey, D. C.; Galbraith, S. M.; Tozer, G. M.; Holder, A. L.; Naylor, M. A.; Nolan, J.; Stratford, M. R. L.; Chaplin, D. J.; Hill, S. A. ZD6126: A novel vascular-targeting agent that causes selective destruction of tumor vasculature. *Cancer Res.* **2002**, *62*, 7247-7253; (c) Hori, K.; Saito, S. Microvascular mechanisms by which the combretastatin A-4 derivative AC7700 (AVE8062) induces tumour blood flow stasis. *Br. J. Cancer* **2003**, *89*, 1334-1344.
  14. (a) Jordan, M. A.; Wilson, L. Microtubules as a target for anticancer drugs. *Nature Rev. Cancer* **2004**, *4*, 253-265; (b) Kanthou, C.; Tozer, G. M. Microtubule depolymerizing vascular disrupting agents: novel therapeutic agents for oncology and other pathologies. *Int. J. Exp. Pathol.* **2009**, *90*, 284-294.
  15. Finkelstein, Y.; Aks, S. E.; Hutson, J. R.; Juurlink, D. N.; Nguyen, P.; Dubnov-Raz, G.; Pollak, U.; Koren, G.; Bentur, Y. Colchicine poisoning: the dark side of an ancient drug. *Clin. Toxicol.* **2010**, *48*, 407-414.
  16. (a) Young, S. L.; Chaplin, D. J. Combretastatin A4 phosphate: background and current clinical status. *Expert. Opin. Invest. Drugs* **2004**, *13*, 1171-1182; (b) Kirwan, I. G.; Loadman, P. M.; Swaine, D. J.; Anthoney, D. A.; Pettit, G. R.; Lippert, J. W.; Shnyder, S. D.; Cooper, P. A.; Bibby, M. C. Comparative preclinical pharmacokinetic and metabolic studies of the combretastatin prodrugs combretastatin A4 phosphate and A1 phosphate. *Clin. Cancer Res.* **2004**, *10*, 1446-1453.



17. Ripphausen, P.; Nisius, B.; Bajorath, J. State-of-the-art in ligand-based virtual screening. *Drug Discov. Today* **2011**, *16*, 372-376.
18. (a) Nicholls, A.; McGaughey, G. B.; Sheridan, R. P.; Good, A. C.; Warren, G.; Mathieu, M.; Muchmore, S. W.; Brown, S. P.; Grant, J. A.; Haigh, J. A.; Nevins, N.; Jain, A. N.; Kelley, B. Molecular Shape and Medicinal Chemistry: A Perspective. *J. Med. Chem.* **2010**, *53*, 3862-3886; (b) Mohammed, M. Z.; Vyjayanti, V. N.; Laughton, C. A.; Dekker, L. V.; Fischer, P. M.; Wilson, D. M.; Abbotts, R.; Shah, S.; Patel, P. M.; Hickson, I. D.; Madhusudan, S. Development and evaluation of human AP endonuclease inhibitors in melanoma and glioma cell lines. *Br. J. Cancer* **2011**, *104*, 653-663.
19. Irwin, J. J.; Sterling, T.; Mysinger, M. M.; Bolstad, E. S.; Coleman, R. G. ZINC: A Free Tool to Discover Chemistry for Biology. *J. Chem. Inf. Model.* **2012**, *52*, 1757-1768.
20. Weininger, D. SMILES, a chemical language and information system.1. Introduction to methodology and encoding rules. *J. Chem. Inf. Comput. Sci.* **1988**, *28*, 31-36.
21. FILTER OpenEye Scientific Software Inc., Santa Fe, NM, USA, [www.eyesopen.com](http://www.eyesopen.com)
22. OMEGA OpenEye Scientific Software Inc., Santa Fe, NM, USA, [www.eyesopen.com](http://www.eyesopen.com).
23. ROCS OpenEye Scientific Software Inc., Santa Fe, NM, USA, [www.eyesopen.com](http://www.eyesopen.com).
24. Grant, J. A.; Gallardo, M. A.; Pickup, B. T. A fast method of molecular shape comparison: A simple application of a Gaussian description of molecular shape. *J. Comput. Chem.* **1996**, *17*, 1653-1666.
25. Rush, T. S.; Grant, J. A.; Mosyak, L.; Nicholls, A. A shape-based 3-D scaffold hopping method and its application to a bacterial protein-protein interaction. *J. Med. Chem.* **2005**, *48*, 1489-1495.
26. Ravelli, R. B. G.; Gigant, B.; Curmi, P. A.; Jourdain, I.; Lachkar, S.; Sobel, A.; Knossow, M. Insight into tubulin regulation from a complex with colchicine and a stathmin-like domain. *Nature* **2004**, *428*, 198-202.
27. Dorleans, A.; Gigant, B.; Ravelli, R. B. G.; Mailliet, P.; Mikol, V.; Knossow, M. Variations in the colchicine-binding domain provide insight into the structural switch of tubulin. *Proc. Natl. Acad. Sci. U. S. A.* **2009**, *106*, 13775-13779.
28. Huang, K. H.; Veal, J. M.; Fadden, R. P.; Rice, J. W.; Eaves, J.; Strachan, J.-P.; Barabasz, A. F.; Foley, B. E.; Barta, T. E.; Ma, W.; Silinski, M. A.; Hu, M.; Partridge, J. M.; Scott, A.; DuBois, L. G.; Freed, T.; Steed, P. M.; Ommen, A. J.; Smith, E. D.; Hughes, P. F.; Woodward, A. R.; Hanson, G. J.; McCall, W. S.; Markworth, C. J.; Hinkley, L.; Jenks, M.; Geng, L.; Lewis, M.; Otto, J.; Pronk, B.; Verleysen, K.; Hall, S. E.

Discovery of Novel 2-Aminobenzamide Inhibitors of Heat Shock Protein 90 as Potent, Selective and Orally Active Antitumor Agents. *J. Med. Chem.* **2009**, *52*, 4288-4305.

29. Brown, S. M.; Bentley, T. W.; Jones, R. O. Process for the preparation of acylated cyclic 1,3-dicarbonyl compounds. WO 99/28282.
30. Barker, J. J.; Barker, O.; Boggio, R.; Chauhan, V.; Cheng, R. K. Y.; Corden, V.; Courtney, S. M.; Edwards, N.; Falque, V. M.; Fusar, F.; Gardiner, M.; Hamelin, E. M. N.; Hesterkamp, T.; Ichihara, O.; Jones, R. S.; Mather, O.; Mercurio, C.; Minucci, S.; Montalbetti, C.; Muller, A.; Patel, D.; Phillips, B. G.; Varasi, M.; Whittaker, M.; Winkler, D.; Yarnold, C. J. Fragment-based Identification of Hsp90 Inhibitors. *ChemMedChem* **2009**, *4*, 963-966.
31. Donkor, I. O.; Li, H.; Queener, S. F. Synthesis and DHFR inhibitory activity of a series of 6-substituted-2,4-diaminothieno 2,3-d pyrimidines. *Eur. J. Med. Chem.* **2003**, *38*, 605-611.
32. Tamura, Y.; Yoshimoto, Y.; Kunimoto, K.; Tada, S.; Tomita, T.; Wada, T.; Seto, E.; Murayama, M.; Shibata, Y.; Nomura, A.; Ohata, K. Nonsteroidal antiinflammatory agents. 1. 5-Alkoxy-3-biphenylacetic acids and related compounds as new potential antiinflammatory agents. *J. Med. Chem.* **1977**, *20*, 709-714.
33. Zhang, W.; Benmohamed, R.; Arvanites, A. C.; Morimoto, R. I.; Ferrante, R. J.; Kirsch, D. R.; Silverman, R. B. Cyclohexane 1,3-diones and their inhibition of mutant SOD1-dependent protein aggregation and toxicity in PC12 cells. *Biorg. Med. Chem.* **2012**, *20*, 1029-1045.
34. Ilic, M.; Ilas, J.; Dunkel, P.; Matyus, P.; Bohac, A.; Liekens, S.; Kikelj, D. Novel 1,4-benzoxazine and 1,4-benzodioxine inhibitors of angiogenesis. *Eur. J. Med. Chem.* **2012**, *58*, 160-170.
35. Liekens, S.; Gijsbers, S.; Vanstreels, E.; Daelemans, D.; De Clercq, E.; Hatse, S. The nucleotide analog cidofovir suppresses basic fibroblast growth factor (FGF2) expression and signaling and induces apoptosis in FGF2-overexpressing endothelial cells. *Mol. Pharmacol.* **2007**, *71*, 695-703.
36. Fortin, S.; Lacroix, J.; Cote, M.-F.; Moreau, E.; Petitclerc, E.; Gaudreault, R. C. Quick and Simple Detection Technique to Assess the Binding of Antimicrotubule Agents to the Colchicine-Binding Site. *Biol. Proced. Online* **2010**, *12*, 113-117.
37. Medrano, F. J.; Andreu, J. M.; Gorbunoff, M. J.; Timasheff, S. N. Roles of colchicine ring-B and ring-C in the binding process to tubulin. *Biochemistry (Mosc)*. **1989**, *28*, 5589-5599.
38. Medrano, F. J.; Andreu, J. M.; Gorbunoff, M. J.; Timasheff, S. N. Roles of ring-C oxygens in the binding of colchicine to tubulin. *Biochemistry (Mosc)*. **1991**, *30*, 3770-3777.

39. Barbier, P.; Peyrot, V.; Leynadier, D.; Andreu, J. M. The active GTP- and ground CDP-Liganded states of tubulin are distinguished by the binding of chiral isomers of ethyl 5-amino-2-methyl-1,2-dihydro-3-phenylpyrido 3,4-b pyrazin-7-yl carbamate. *Biochemistry (Mosc)*. **1998**, *37*, 758-768.
40. Barbier, P.; Dorleans, A.; Devred, F.; Sanz, L.; Allegro, D.; Alfonso, C.; Knossow, M.; Peyrot, V.; Andreu, J. M. Stathmin and Interfacial Microtubule Inhibitors Recognize a Naturally Curved Conformation of Tubulin Dimers. *J. Biol. Chem.* **2010**, *285*, 31672-31681.
41. Medrano, F. J.; Andreu, J. M.; Gorbunoff, M. J.; Timasheff, S. N. Roles of ring C oxygens in the binding of colchicine to tubulin. *Biochemistry* **1991**, *30*, 3770-7.
42. Díaz, J. F.; Buey, R. M., Characterizing Ligand-Microtubule Binding by Competition Methods. In *Methods in Molecular Medicine*, Zhou, J., Ed. Humana Press Inc.: Totowa, NJ, 2007; Vol. 137, pp 245-260.
43. Leynadier, D.; Peyrot, V.; Sarrazin, M.; Briand, C.; Andreu, J. M.; Renner, G. A.; Temple, C., Jr. Tubulin binding of two 1-deaza-7,8-dihydropteridines with different biological properties: enantiomers NSC 613862 (S)-(-) and NSC 613863 (R)-(+). *Biochemistry* **1993**, *32*, 10675-82.
44. Xu, K.; Schwarz, P. M.; Luduena, R. F. Interaction of nocodazole with tubulin isotypes. *Drug Dev. Res.* **2002**, *55*, 91-96.
45. Cortese, F.; Bhattacharyya, B.; Wolff, J. Podophyllotoxin as a probe for colchicine binding-site of tubulin. *J. Biol. Chem.* **1977**, *252*, 1134-1140.
46. Diaz, J. F.; Andreu, J. M. Kinetics of dissociation of the tubulin-colchicine complex - Complete reaction scheme and comparison to thermodynamic measurements. *J. Biol. Chem.* **1991**, *266*, 2890-2896.
47. Mooberry, S. L.; Weiderhold, K. N.; Dakshanamurthy, S.; Hamel, E.; Banner, E. J.; Kharlamova, A.; Hempel, J.; Gupton, J. T.; Brown, M. L. Identification and characterization of a new tubulin-binding tetrasubstituted brominated pyrrole. *Mol. Pharmacol.* **2007**, *72*, 132-140.
48. Andreu, J. M., Tubulin Purification. In *Methods in Molecular Medicine*, Zhou, J., Ed. Humana Press Inc.: Totowa, NJ, 2007; Vol. 137, pp 17-28.
49. Fitzgerald, T. J. Molecular features of colchicine associated with antimitotic activity and inhibition of tubulin polymerization. *Biochem Pharmacol* **1976**, *25*, 1383-7.
50. Temple, C.; Renner, G. A.; Comber, R. N. New anticancer agents - Alterations of the carbamate group of ethyl (5-amino-1,2-dihydro-3-phenylpyrido-3,4-b-pyrazin-7-yl)carbamates. *J. Med. Chem.* **1989**, *32*, 2363-2367.



**Figure 1.** Chemical structures of selected colchicine-site binders

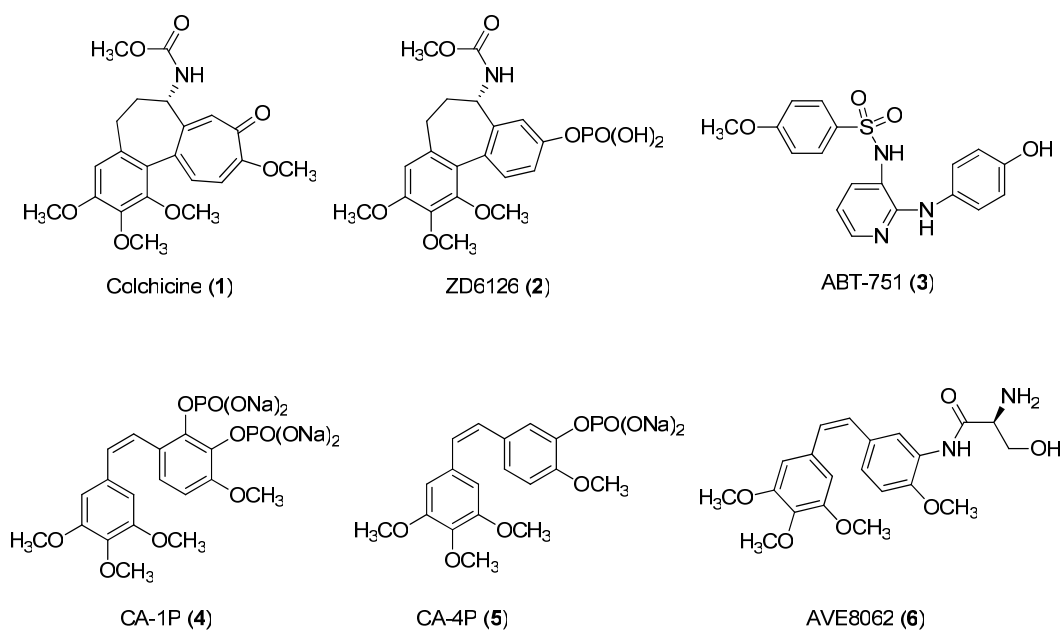


**Figure 2.** Schematic view of the virtual screening protocol

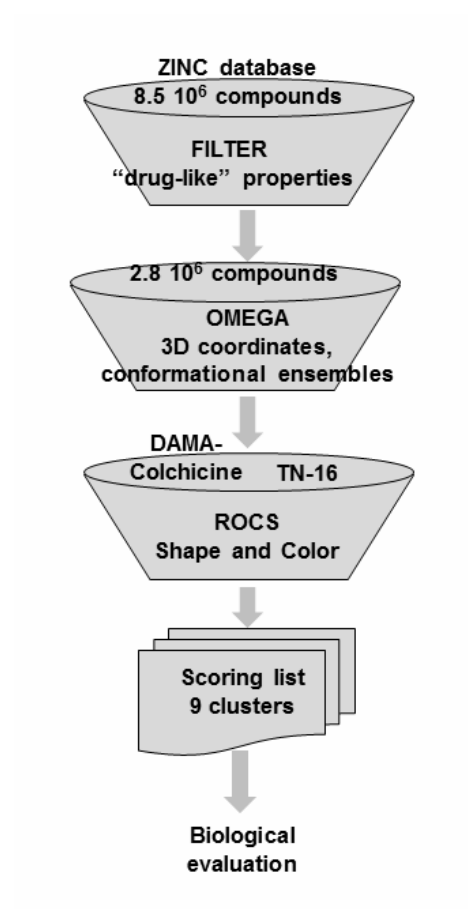
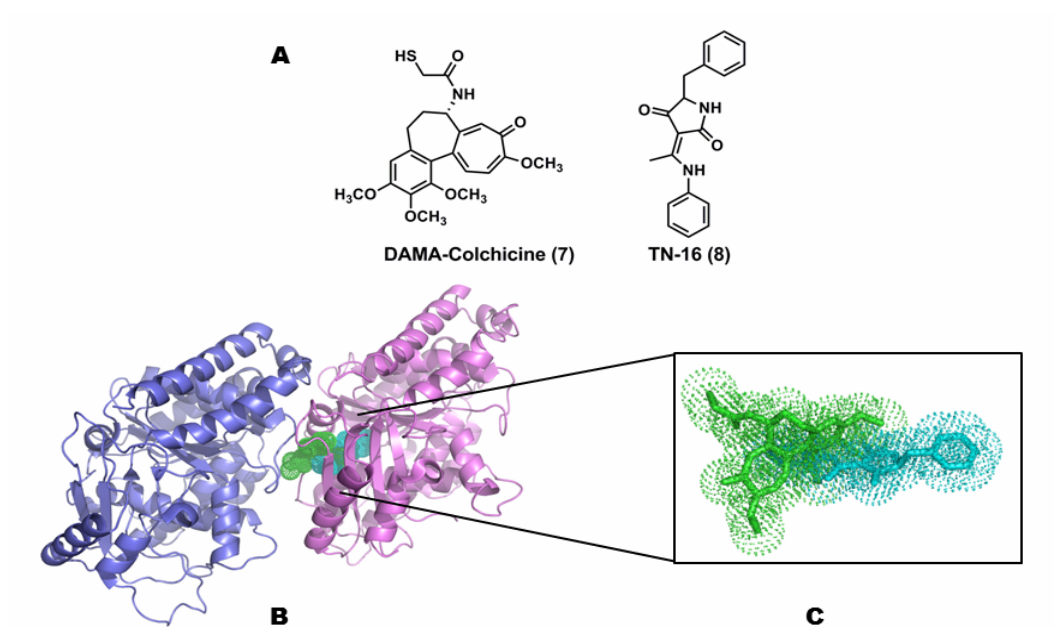


**Figure 3**



A. Chemical structures of DAMA-colchicine (7) and TN-16 (8). B. Colchicine binding-site in the  $\alpha,\beta$ -tubulin dimer. C. Superposition of the ligands used in the VS: DAMA-colchicine (green, pdb 1sa0) and TN-16 (cyan, pdb 3hkd).

**Figure 4.** Structure of the hit compound **9** identified from the VS campaign.

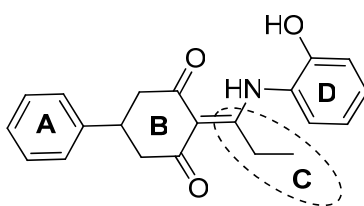
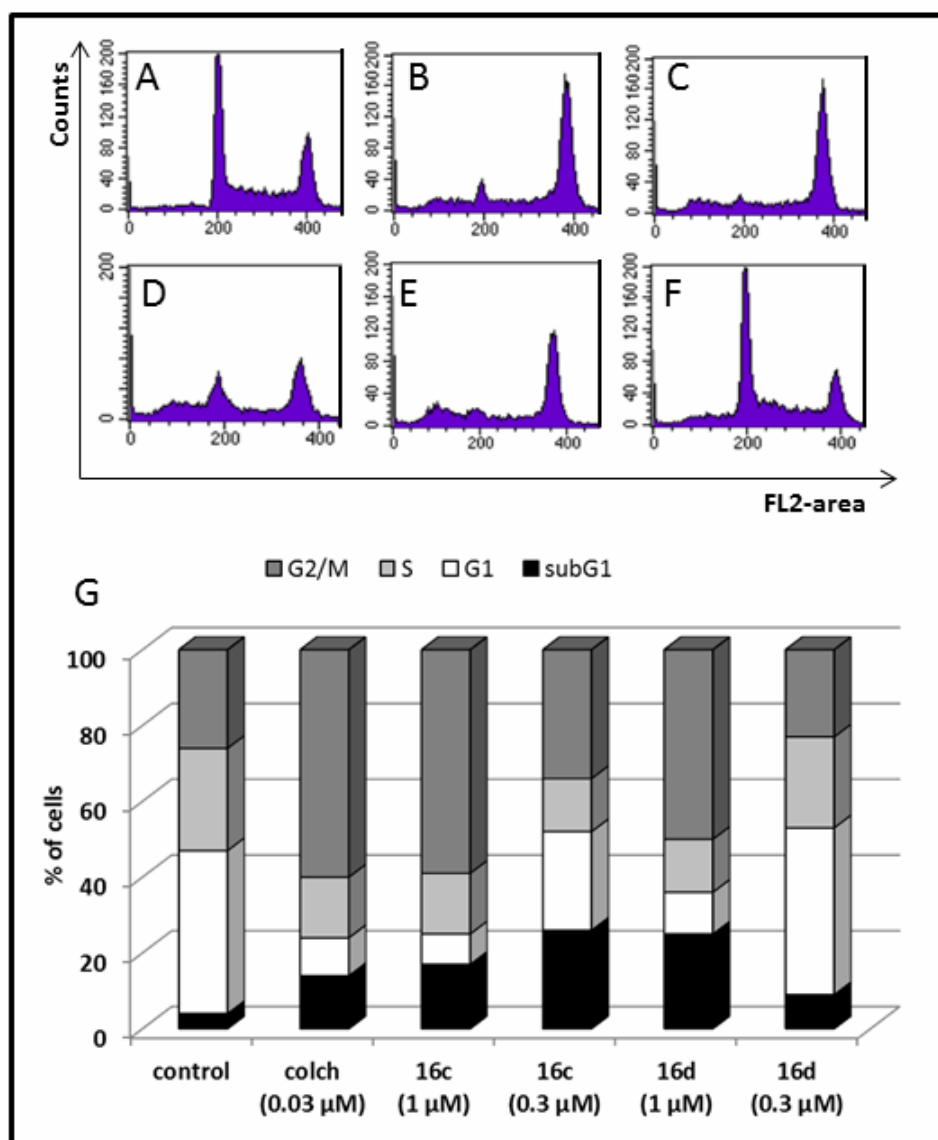


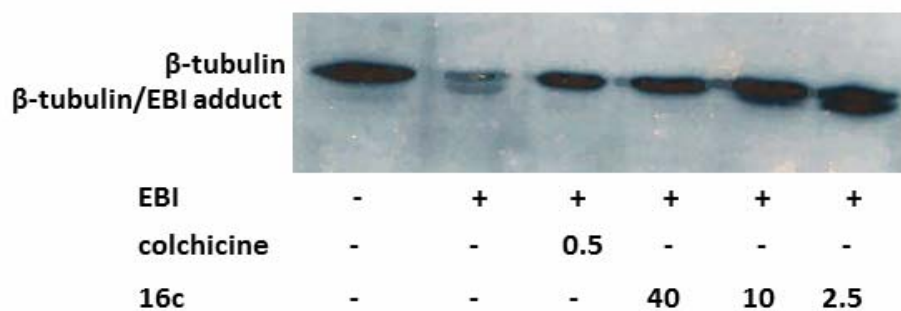


**Figure 5.**



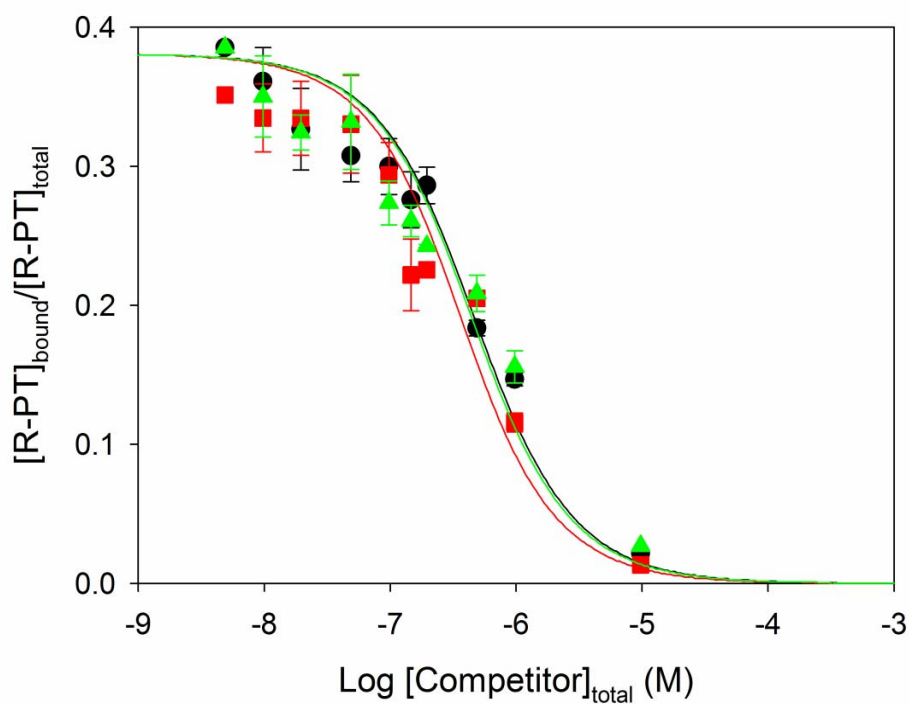
**Cell cycle distribution.** HMEC-1 were treated with DMSO (A), colchicine (0.03  $\mu$ M, B), **16c** (1  $\mu$ M, C or 0.3  $\mu$ M, D) or **16d** (1  $\mu$ M, E or 0.3  $\mu$ M, F) for 24 h. Next, the cells were harvested, stained with propidium iodide, and cell cycle distribution was evaluated by flow cytometry. Percentages of cells in the different phases of the cell cycle are indicated (G).

**Figure 6.**



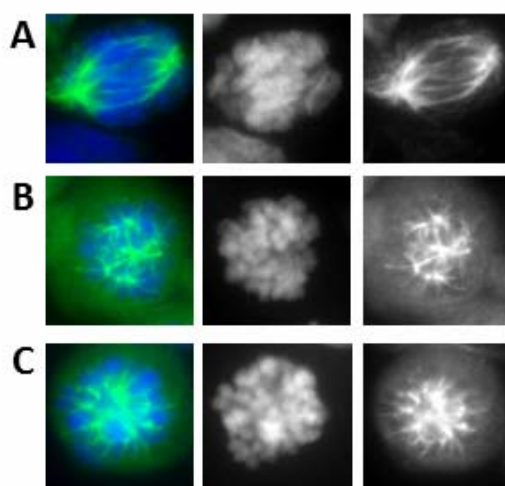
**Inhibition of tubulin binding by 16c.** MDA-MB-231 cells were treated with DMSO, colchicine ( 0.5  $\mu$ M) or **16c** (40, 10 or 2.5  $\mu$ M) for 16 h. Next EBI (100  $\mu$ M) was added and after 1.5 h, the cells were harvested and cell extracts were prepared for western blot analysis using anti- $\beta$ -tubulin antibody. EBI cross-links cysteine residues in  $\beta$ -tubulin resulting in the formation of a  $\beta$ -tubulin adduct (second immunoreactive band) that migrates faster than  $\beta$ -tubulin. Compounds that bind to the colchicine-binding site in  $\beta$ -tubulin prevent the formation of the EBI: $\beta$ -tubulin adduct.

**Figure 7.**



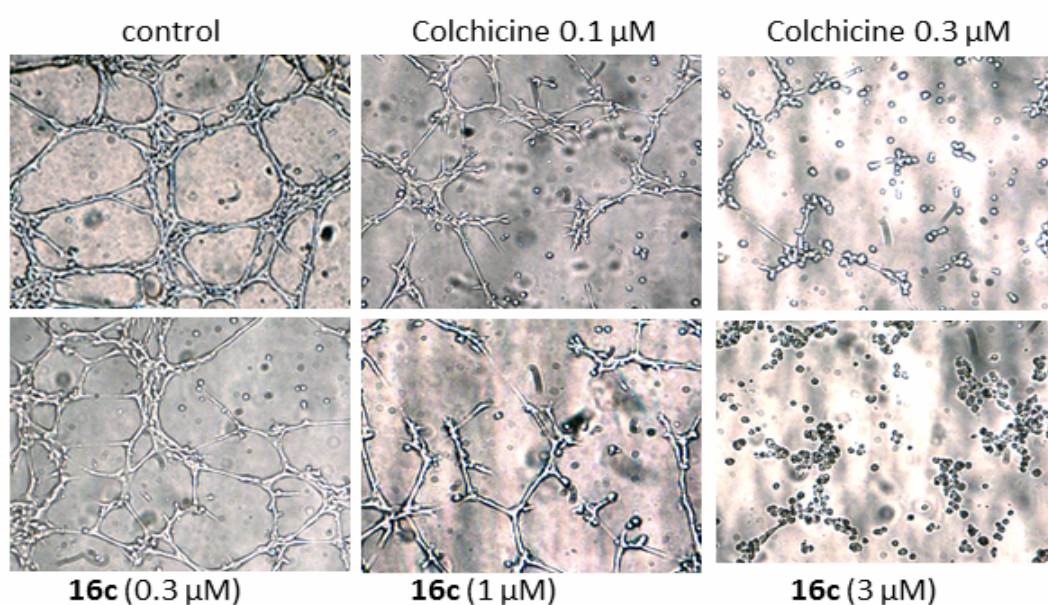
Displacement of the fluorescent probe R-PT (0.2 μM) bound to tubulin (0.2 μM) by **14c** (black lines and circles), **16c** (red lines and squares) and **26f** (green lines and triangles) at 25 °C. The solid lines were generated with the best fit value of the binding equilibrium constant of the competitors, assuming a one-to-one binding to the same site.

**Figure 8.**



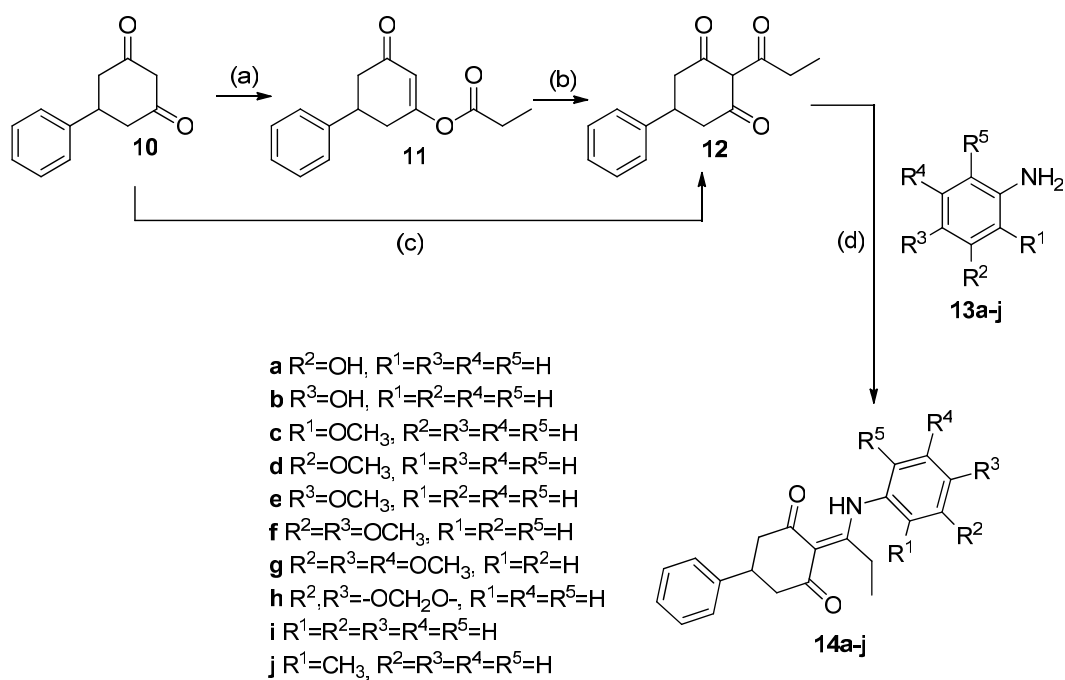
**Inhibition of mitotic spindle formation.** MDA-MB-231 cells were treated for 8 h with DMSO (A), colchicine (0.1  $\mu$ M, B) or **16c** (1  $\mu$ M, C) fixed and stained with anti- $\beta$ -tubulin antibody (green) to visualize the microtubules and DAPI for DNA (blue). Column 1: double staining; column 2: DNA staining only; column 3:  $\beta$ -tubulin staining only.

**Figure 9.**



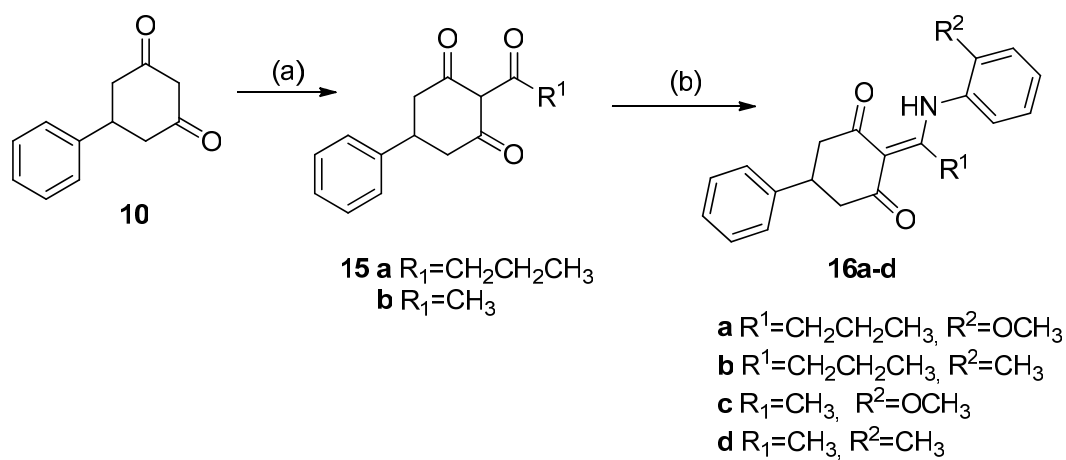
**Vascular disrupting effects of 16c.** HMEC-1 cells were cultured on matrigel for 3 h to allow the formation of tube-like structures. Then DMSO 0.1% (control), colchicine (0.1 or 0.3  $\mu\text{M}$ ) or **16c** (0.3, 1 or 3  $\mu\text{M}$ ) were added. Images show the vascular network after 90 min of treatment.

**Scheme 1<sup>a</sup>**



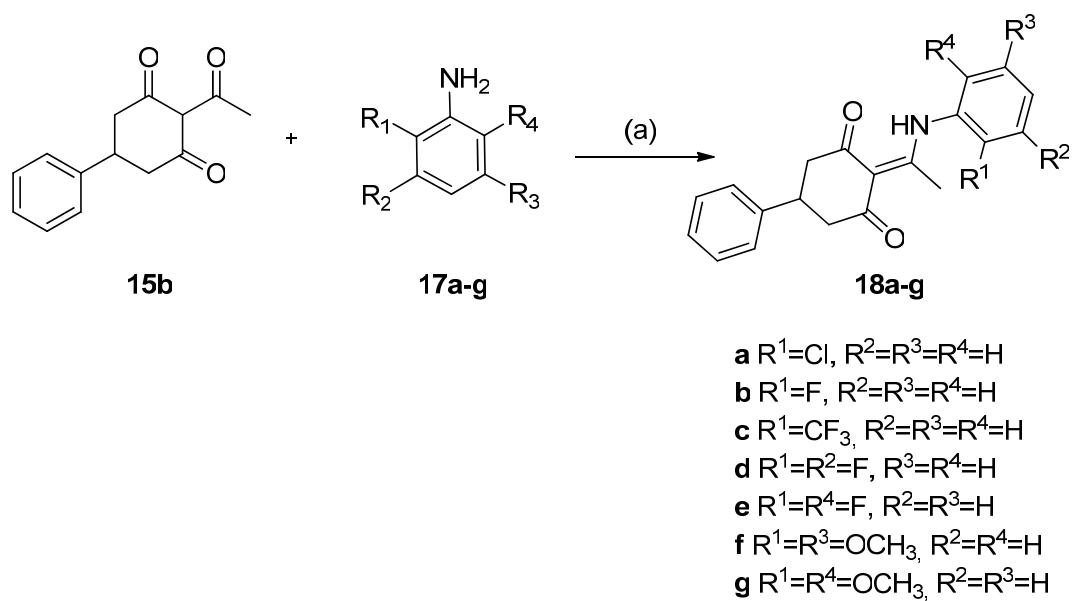
<sup>a</sup> Reagents and conditions: (a) DMAP, DIPEA,  $CH_2Cl_2$ , 70 °C, 2 h, 64% yield; (b)  $K_2CO_3$  anh., 1,2,4-triazole,  $CH_3CN$ , 30 °C, > 48 h, 30% yield; (c)  $K_2CO_3$  anh., 1,2,4-triazole,  $Bu_4NBr$ ,  $CH_3CN$ , MW, 70 °C, 2 h, 51% yield. (d) Toluene, 4Å molecular sieves, MW, 150 °C, 2 h, 30-98% yields.

**Scheme 2<sup>a</sup>**



<sup>a</sup> Reagents and conditions: (a)  $R^1\text{COCl}$ ,  $\text{K}_2\text{CO}_3$  anh, 1,2,4-triazole,  $\text{Bu}_4\text{NBr}$ ,  $\text{CH}_3\text{CN}$ , MW,  $70^\circ\text{C}$ , 2 h (**15a**, 29% yield; **15b**, 54% yield); (b) substituted aniline, toluene, molecular sieves, MW,  $150^\circ\text{C}$ , 2 h, 60-84% yields.

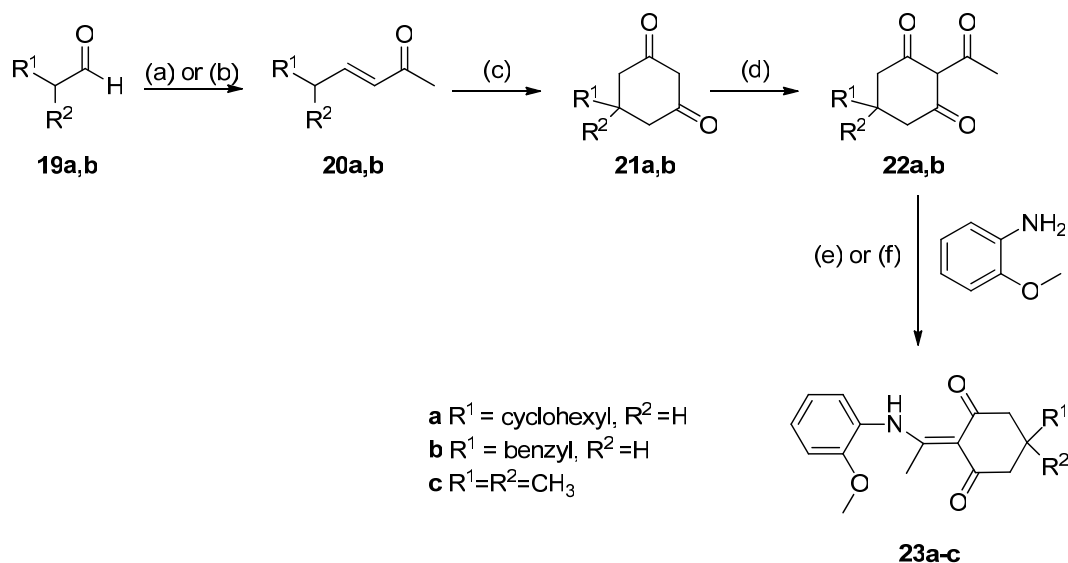
**Scheme 3<sup>a</sup>**



<sup>a</sup> Reagents and conditions: (a) toluene, molecular sieves, MW, 150 °C, 2 h, 23-78% yields.

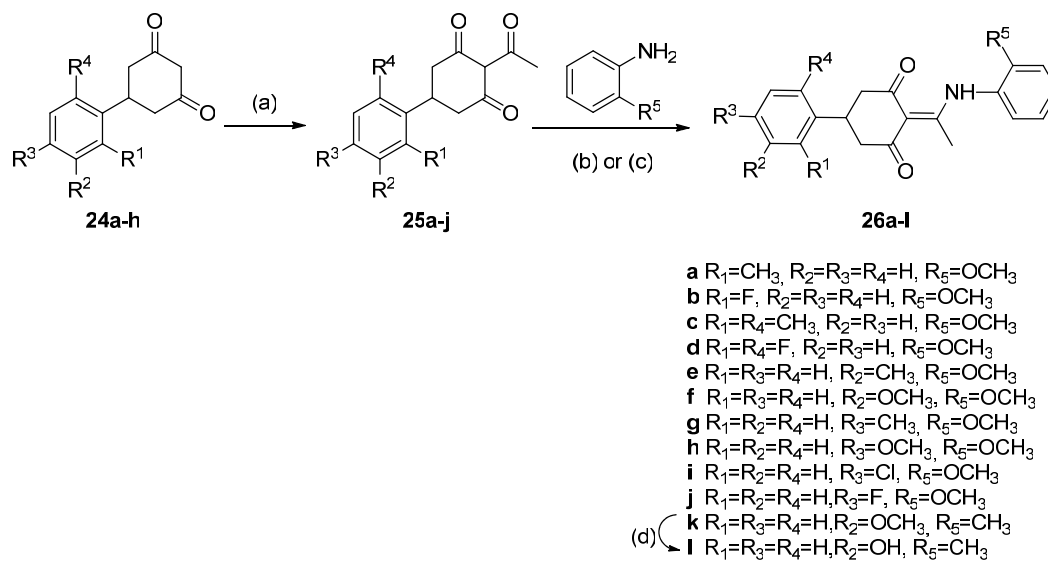


**Scheme 4<sup>a</sup>**



<sup>a</sup> Reagents and conditions: (a) NaOH (1%), acetone, H<sub>2</sub>O, rt, overnight (for **20a**, 65% yield); (b) Ph<sub>3</sub>P=CHCOCH<sub>3</sub>, CHCl<sub>3</sub>, 60 °C, 4 h (for **20b**, 77% yield); (c) (i) Diethyl malonate, EtONa, EtOH, Δ; (ii) NaOH, 80 °C, 2 h; (iii) HCl, Δ, 1 h (**21a** 69% yield, **21b** 33% yield); (d) ClCOCH<sub>3</sub>, K<sub>2</sub>CO<sub>3</sub> anh, 1,2,4-triazole, Bu<sub>4</sub>NBr, CH<sub>3</sub>CN, MW, 70 °C, 2 h (**22a** 36% yield, **22b** 38% yield, **22c** was commercially available); (e) toluene, molecular sieves, pressure tube, 110 °C, overnight (for **23a** 89% yield, for **23b** 73% yield); (f) toluene, molecular sieves, MW, 150 °C, 2 h (for **23c** 79% yield).

**Scheme 5<sup>a</sup>**



<sup>a</sup> Reagents and conditions: (a)  $CH_3COCl$ ,  $K_2CO_3$  anh, 1,2,4-triazole,  $Bu_4NBr$ ,  $CH_3CN$ , MW, 70 °C, 2 h, 14-74% yields; (b) For **26e-j**: toluene, molecular sieves, MW 150 °C, 2 h, 39-99% yields; (c) For **26a-d,k**: toluene, molecular sieves, pressure tube, 110 °C, overnight, 39-75% yields; (d)  $BBr_3$ ,  $CH_2Cl_2$ , rt, 12 h, 23% yield.

**Table 1. Anti-proliferative activity of compounds 14a-j, 16a-d and 18a-g in endothelial and tumor cell lines**

Compound	Endothelial cells IC <sub>50</sub> (μM)			Tumor cells IC <sub>50</sub> (μM)		
	HMEC-1	MBEC	BAEC	L1210	CEM	HeLa
<b>Colchicine</b>	0.0038 ± 0.0011	0.031 ± 0.015	0.0069 ± 0.0008	0.010 ± 0.001	0.013 ± 0.001	0.0087 ± 0.0001
<b>9</b>	22 ± 13	13 ± 5	35 ± 1	13 ± 1	15 ± 9	11 ± 8
<b>14a</b>	13 ± 6	12 ± 3	7.8 ± 0.9	15 ± 12	48 ± 26	75 ± 25
<b>14b</b>	28 ± 21	18 ± 0	36 ± 2	14 ± 7	34 ± 0	79 ± 42
<b>14c</b>	1.4 ± 0.2	1.4 ± 0.1	1.2 ± 0.6	1.5 ± 0.2	2.3 ± 1.7	4.3 ± 0.7
<b>14d</b>	18 ± 9	16 ± 4	64 ± 14	32 ± 9	45 ± 12	66 ± 9
<b>14e</b>	≥ 100	57 ± 7	≥ 100	58 ± 13	67 ± 11	≥ 100
<b>14f</b>	> 100	> 100	> 100	> 100	> 100	> 100
<b>14g</b>	> 100	> 100	> 100	> 100	> 100	> 100
<b>14h</b>	53 ± 11	50 ± 18	43 ± 6	38 ± 0	53 ± 22	76 ± 5
<b>14i</b>	15 ± 6	8.3 ± 2.1	16 ± 11	22 ± 17	21 ± 11	56 ± 3
<b>14j</b>	2.1 ± 2.0	2.8 ± 0.2	2.2 ± 0.2	6.9 ± 1.5	6.3 ± 1.2	9.2 ± 5.0
<b>16a</b>	31 ± 3	27 ± 4	16 ± 3	36 ± 8	41 ± 1	59 ± 23
<b>16b</b>	44 ± 2	47 ± 3	46 ± 4	41 ± 19	≥ 100	> 100
<b>16c</b>	0.09 ± 0.01	0.12 ± 0.01	0.09 ± 0.01	0.16 ± 0.08	0.18 ± 0.05	0.18 ± 0.00
<b>16d</b>	0.26 ± 0.08	0.32 ± 0.04	0.17 ± 0.03	0.30 ± 0.18	0.68 ± 0.09	0.48 ± 0.26
<b>18a</b>	0.56 ± 0.16	0.47 ± 0.05	0.29 ± 0.03	0.70 ± 0.62	0.64 ± 0.18	0.71 ± 0.20
<b>18b</b>	0.93 ± 0.46	1.0 ± 0.1	0.51 ± 0.01	1.9 ± 0.7	1.1 ± 0.3	3.4 ± 2.4
<b>18c</b>	7.7 ± 2.1	8.7 ± 0.1	8.1 ± 0.5	14 ± 10	18 ± 2	32 ± 18
<b>18d</b>	10 ± 2	12 ± 0	14 ± 2	19 ± 1	25 ± 18	36 ± 3
<b>18e</b>	6.6 ± 0.5	9.2 ± 1.8	8.4 ± 1.5	11 ± 2	21 ± 6	17 ± 4
<b>18f</b>	2.6 ± 0.2	3.2 ± 0.2	2.6 ± 0.5	36 ± 22	6 - >100*	46 ± 3

<b>18g</b>	$1.4 \pm 0.8$	$1.2 \pm 0.2$	$0.46 \pm 0.29$	$1.0 \pm 0.0$	$1.4 \pm 0.7$	$1.1 \pm 0.2$
------------	---------------	---------------	-----------------	---------------	---------------	---------------

---

\*Indicates no dose response in the indicated concentration range, making accurate IC<sub>50</sub> calculation impossible

**Table 1 (cont) . Anti-proliferative activity of compounds 23a-c and 26a-l in endothelial and tumor cell**

**lines**

Compound	Endothelial cells				Tumor cells	
	IC <sub>50</sub> (μM)				IC <sub>50</sub> (μM)	
	HMEC-1	MBEC	BAEC	L1210	CEM	HeLa
<b>Colchicine</b>	0.0038 ± 0.0011	0.031 ± 0.015	0.0069 ± 0.0008	0.010 ± 0.001	0.013 ± 0.001	0.0087 ± 0.0001
<b>23a</b>	12 ± 1	21 ± 5	12 ± 1	8 - >100*	15 ± 6	11 ± 5
<b>23b</b>	22 ± 2	87 ± 15	>100	>100	>100	>100
<b>23c</b>	76 ± 18	71 ± 41	48 ± 11	>100	>100	>100
<b>26a</b>	5.8 ± 0.4	6.8 ± 0.8	3.2 ± 0.2	11 ± 0	7.2 ± 0.2	13 ± 3
<b>26b</b>	4.3 ± 0.3	5.4 ± 0.6	2.7 ± 0.2	6.3 ± 0.6	4.9 ± 1.4	4.8 ± 0.1
<b>26c</b>	35 ± 1	39 ± 2	41 ± 2	24 ± 3	23 ± 0	55 ± 27
<b>26d</b>	39 ± 8	60 ± 9	>100	>100	>100	>100
<b>26e</b>	0.33 ± 0.12	0.42 ± 0.01	0.26 ± 0.07	0.17 ± 0.11	0.31 ± 0.07	0.79 ± 0.12
<b>26f</b>	0.30 ± 0.08	0.41 ± 0.08	0.23 ± 0.09	0.21 ± 0.09	0.24 ± 0.10	0.69 ± 0.01
<b>26g</b>	11 ± 3	9.2 ± 1.1	8.4 ± 0.2	>100	>100	90 ± 4
<b>26h</b>	>100	>100	>100	>100	>100	>100
<b>26i</b>	55 ± 16	46 ± 1	42 ± 1	22 ± 0	28 ± 8	58 ± 23
<b>26j</b>	1.8 ± 0.1	2.1 ± 0.1	1.7 ± 0.4	3.3 ± 0.4	5.3 ± 1.0	4.0 ± 0.4
<b>26k</b>	0.67 ± 0.07	0.64 ± 0.05	0.48 ± 0.04	0.26 ± 0.22	0.72 ± 0.25	0.66 ± 0.03
<b>26l</b>	2.2 ± 0.6	2.5 ± 0.2	2.1 ± 0.1	3.5 ± 1.7	6.2 ± 0.2	4.1 ± 0.2

\*Indicates no dose response in the indicated concentration range, making accurate IC<sub>50</sub> calculation impossible

**Table 2. Association constants for compounds 14c, 16c and 26f and other colchicine-binding site ligands**

<b>Compound</b>	<b><math>K_{\text{assoc}}</math> (<math>\text{M}^{-1}</math>) 25°C</b>
<b>Colchicine</b>	$1.16 \times 10^7$ (at 37°C) <sup>a</sup>
<b>MTC</b>	$4.7 \times 10^5$ <sup>b</sup>
<b>R-PT</b>	$3.2 \times 10^6$ <sup>c</sup>
<b>Podofilotoxin</b>	$1.8 \times 10^6$ <sup>d</sup>
<b>Nocodazole</b>	$4 \times 10^5$ <sup>e</sup>
<b>14c</b>	$(7.1 \pm 1.2) \times 10^6$
<b>16c</b>	$(9.6 \pm 1.2) \times 10^6$
<b>26f</b>	$(7.5 \pm 0.76) \times 10^6$

<sup>a</sup>Data from ref. 46. <sup>b</sup>Data from ref. 40 <sup>c</sup>Data from ref. 43. <sup>d</sup>Data from ref. 45. <sup>e</sup>Data from ref. 44.

Table of contents graphic

**Novel vascular disrupting agents with a cyclohexanedione scaffold identified through a ligand-based virtual screening approach**

*María-Dolores Canela, María-Jesús Pérez-Pérez, Sam Noppen, Gonzalo Sáez-Calvo, J. Fernando Díaz, María-José Camarasa, Sandra Liekens and Eva-María Priego.*

